Microsystem Technologies (2022) 28:1143–1165
https://doi.org/10.1007/s00542-022-05272-1

TECHNICAL PAPER

Structural dynamic responses of layer-by-layer viscoelastic sandwich nanocomposites subjected to time-varying symmetric thermal shock loadings based on nonlocal thermo-viscoelasticity theory

Huili Guo[1,3] · Lu Yaning[1] · Chenlin Li[1,3] · Tianhu He[2]

Received: 21 April 2021 / Accepted: 28 February 2022 / Published online: 19 March 2022

Abstract

The layer-by-layer viscoelastic sandwich nanocomposites have been widely used as high-efficient shock absorbers in nano-engineering since its excellent performance in vibration isolation. Such structure often works in thermoelastic coupling condition, and a thorough and comprehensive investigation on its structural dynamic responses is imperatively needed to achieve the goal of improving heat isolation and avoiding unwanted vibration. In this work, an analytical study is conducted to investigate the structural dynamic responses of layer-by-layer viscoelastic sandwich nanocomposites based on nonlocal thermo-viscoelasticity theory. The two lateral bounding surfaces of the structure are subjected to the time-varying symmetric thermal shock loadings. It is assumed that thermal contact resistance and elastic wave impedance at the interface are zero with idealized adhesion. Governing equations of each homogeneous isotropic viscoelastic layer are derived and solved by a semi-analytical technique via Laplace transformation. The achieved results show that the heat isolation will be maximally improved and harmful thermal induced stress is lowered to some extent if properly selecting nonlocal parameters and material constants ratios.

List of symbols

$\rho^{(i)}$	Mass density
$\lambda^{(i)}$, $\mu^{(i)}$	Lame's constants
T_0	Reference temperature
$K_0^{(i)}$	Bulk modulus
$c_E^{(i)}$	Specific heat at constant strain
$\Gamma()$	Gamma function
$H()$	Heaviside function
$\alpha_T^{(i)}$	Coefficient of linear thermal expansion
$\kappa^{(i)}$	Coefficient of thermal conductivity
$w^{(i)}$	Components of displacement vector in the z-direction
$\theta^{(i)}$	Temperature increment
$\sigma_{zz}^{(i)}$	Component of stress tensor in the z-direction
$\varepsilon_{zz}^{(i)}$	Component of strain tensor in the z-direction
$q_z^{(i)}$	Components of heat flux vector in the z-direction
$S^{(i)}$	Entropy density
$\overline{\chi}_q^{(i)}$	Thermal nonlocal parameter
$\overline{e}_0\overline{a}^{(i)}$	Elastic nonlocal parameter

✉ Chenlin Li
liguomechanics@163.com

1 School of Civil Engineering, Lanzhou Jiaotong University, Lanzhou 730070, Gansu, People's Republic of China

2 School of Science, Lanzhou University of Technology, Lanzhou 730050, Gansu, People's Republic of China

3 State Key Laboratory for Strength and Vibration of Mechanical Structures, Xi'an Jiaotong University, Xi'an 710049, Shaanxi, People's Republic of China

1 Introduction

Viscoelastic sandwich composites stand as a class of efficient damping structures which have been widely used in passive vibration control systems (Akbarov et al. 2014; Sheng et al. 2018; Li et al. 2018). In recent years, the rapid development of viscoelastic materials (Zhou et al. 2016) leads to extensive applications of viscoelastic sandwich composites. Since the discovery of new viscoelastic nanomaterials (e.g., ethylene glycol-Al_2O_3, etc.), viscoelastic sandwich nanocomposites becomes one of the most promising candidates for next-generation vibration damping structures, nano-sensors, and nano-actuators. In actual engineering, such structure often serves in a thermoelastic coupling condition, where heat transfer and thermal induced stress will be accompanied. In such a case, its structural dynamic responses to the external thermal shock loadings need to be seriously studied. However, in view of current works, the following questions remain unsolved. Firstly, analytical model of nonlocal thermo-viscoelastic coupling for such structure still has not been developed. Secondly, the influences of size effects of inherent elastic deformation and heat transfer on structural dynamic responses are still not clear. Consequently, it needs to contribute significant efforts to address these problems, which will be beneficial to the safe functioning and vibration control of such structure in the thermoelastic condition. This forms the main objective of the current research.

At the nanoscale, the classical or non-Fourier thermo-viscoelastic models should be further extended by introducing the intrinsic size effects of elastic deformation and heat transfer and additional material size-dependent characteristic lengths. Firstly, the classical viscoelasticity models (e.g., Maxwell model, Voigt model, Zener model, etc.) (Gurtin and Sternberg 1962; Zhou et al. 2016) should be modified by considering material microstructure (Govindjee and Sackman 1999). To characterize mechanical properties of viscoelastic nanomaterials, Eringen's nonlocal elastic stress field theory (Eringen 1972, 1983, 2002) with additional material internal length scale is often used. This continuum-mechanical model is more applicable than the molecular dynamics simulation, which is only valid to nano-systems with limited number of atoms or molecules. Thereafter, some other nonlocal continuum-based elasticity models have been developed to consider size effect of elastic deformation (Polizzotto 2014; Mindlin 1965; Yang et al. 2002; Lim et al. 2015; Li et al. 2019; Li et al. 2021b; Guo et al. 2021a, b; Li et al. 2022), whilst investigations on the mechanical behaviors of nano structures were also performed (Li and Hu, 2015, 2016). In addition, it needs to be emphasized that Eringen's nonlocal differential model is only an approximate one, and some scholars pointed out that this model will be ill-posed in some specific cases (Romano and Barretta 2017; Romano et al. 2017; Barretta and de Sciarra 2018; Zhu and Li 2017). Enlightened by Eringen's works, nonlocal viscoelasticity model has been further developed by introducing size-dependent characteristic length (Lei et al. 2013; Kolahchi 2017; Li et al. 2019).

Secondly, the application of classical heat conduction model will be questionable at the nanoscale. Jou et al. (2010) suggested that the size effect of heat transport will be significant if mean free path of heat carriers becomes comparable to or longer than the characteristic length of the system. Such effect was also verified by an experimental study (Chan et al. 2008), which measures the melting dynamics of silver following femtosecond laser excitation by optical third-harmonic generation. More importantly, some celebrated scholars (Sobolev 1994; Tzou and Guo 2010) believed that the size-dependent heat transport models should be extended by introducing additional material characteristic length. So far, there have been many papers that contributed significant efforts to develop size-dependent heat transfer models, for examples, GK model (Guyer and Krumhans1966), thermomass model (Cao and Guo 2007; Guo and Hou 2010), ballistic-diffusive model (Chen 2001), and collectively diffusive model (Hoogeboom-Pot et al. 2015). Inspired by Eringen's nonlocal stress field theory and nonlocal heat conduction model, Li et al. (2021a) fully considered size effects of elastic strain and thermal fields to develop a complete nonlocal model of thermo-viscoelasticity to provide a thorough and comprehensive understanding on the thermo-mechanical coupling of viscoelastic nanomaterials. In this work, Li et al. used this model to investigate structural dynamic responses of bi-layered composite viscoelastic nanoplate with non-idealized interfacial conditions.

As the above literature survey and further examination of other available works reveal, no work has thoroughly investigated the dynamic thermo-mechanical responses of layer-by-layer viscoelastic sandwich nanocomposites by considering size effects and material constants ratios. To deal with the problem, present work aims to study structural dynamic responses of such structure, of which upper and lower bounding surfaces subjected to time-varying symmetric thermal shock loadings. The thermal contact resistance and elastic wave impedance are assumed to be zero at the interfaces of two adjacent layers. In the context of nonlocal thermo-viscoelasticity theory (Li et al. 2020), the governing equations are derived for isotropic homogeneous viscoelastic layer and are solved by a semi-analytical method via Laplace transformation. The effects of nonlocal parameters and material constants ratios on structural nonlocal thermo-viscoelastic responses are evaluated and illustrated graphically. Finally, some concluding remarks are summarized.

2 Modeling of layer-by-layer viscoelastic sandwich nanocomposites subjected to time-varying symmetric thermal shock loadings

Nano-plate stands as a key component nano-enegineering which has been widely used in various material systems without and in the presence of the thermal field (Kolahchi et al. 2016; Kiani 2016a, b, 2017; Hosseini 2017; Shahrbabaki 2018; Karami and Shahsavari 2019; Biswas 2020). Recently, layer-by-layer viscoelastic sandwich nanocomposites works in thermoelastic coupling condition, and the structural dynamic responses analysis of such structure is of great importance for its vibration control and thermal management. In this section, an analytical model of layer-by-layer viscoelastic sandwich nanoplates composed of two kinds of viscoelastic materials will be investigated.

It is assumed that the structure is initially quiescent. The rectangular coordinate system (x, y, z) is chosen. The thickness of two lateral viscoelastic layers is set as $h^{(\mathrm{I})}$ ($h^{(\mathrm{III})}$) and the middle one is valued as $h^{(\mathrm{II})}$. It is assumed that the thickness of the structure in z-direction is much smaller than its dimension in y- and x-axial direction (i.e. $h_z << h_y$ and $h_z << h_x$). Additionally, thermal contact resistance and elastic wave impedance at the interfaces are zero. It is known that van der Waals forces (i.e., the weak forces that contribute to intermolecular bounding between molecules) can be considered in the vibration analysis of nano-structures (Pradhan and Phadikar 2009; Mahmoudpour et al. 2018; Dowlati and Rezazadeh 2018; Fan and Kiani 2021). Furthermore, it needs to be emphasized that this work mainly contributes to evaluate the size-effects of elastic deformation and heat transfer on the structural dynamic thermo-mechanical responses of layer-by-layer viscoelastic nanoplates. Similar to the work of Yu et al. (2016), the van der Waals forces will be neglected in this paper. In addition, the upper and lower bounding surfaces are considered to be traction free and subjected to time-varying symmetric thermal shock loadings. During the analysis, only the thermo-viscoelastic responses along thickness direction will be studied, so the problem considered in this section can be viewed as a one-dimensional

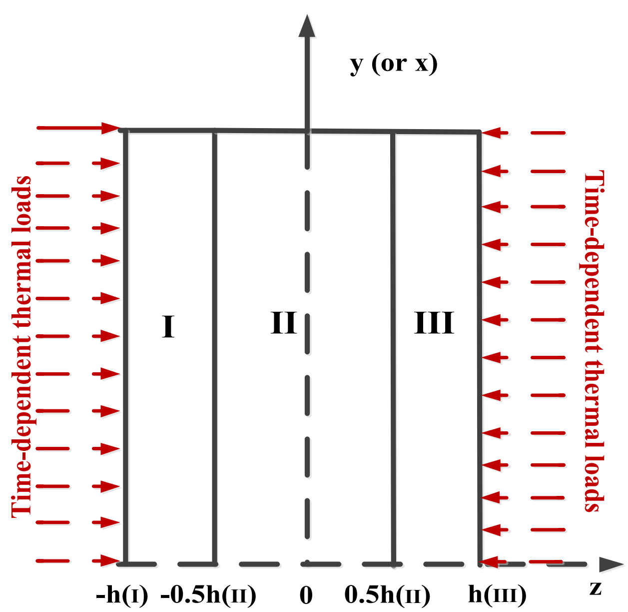

Fig. 1 The schematic model of layer-by-layer viscoelastic sandwich nanoplates subjected to time-varying symmetric thermal shock loadings

problem (see Fig. 1). Consequently, all the physical variables only depend on z and t. The components of displacement and temperature can be expressed as:

$$u_x^{(i)} = 0, \quad u_y^{(i)} = 0, \quad u_z^{(i)} = w^{(i)}(z, t), \quad \theta^{(i)} = \theta^{(i)}(z, t). \tag{1}$$

Initial conditions are:

$$w^{(i)}(z,0) = \dot{w}^{(i)}(z,0) = 0, \quad \theta^{(i)}(z, 0) = \dot{\theta}^{(i)}(z, 0) = 0. \tag{2}$$

Boundary conditions are:

$$\sigma_{zz}^{(\mathrm{I})}\left(\pm h^{(\mathrm{I})},t\right) = 0, \quad \theta^{(\mathrm{I})}\left(\pm h^{(\mathrm{I})},t\right) = f(t). \tag{3}$$

Interfacial conditions are:

$$\begin{aligned} w^{(\mathrm{I})}\big|_{z=-0.5h^{(\mathrm{II})}} &= w^{(\mathrm{II})}\big|_{z=-0.5h^{(\mathrm{II})}}, \\ w^{(\mathrm{II})}\big|_{z=0.5h^{(\mathrm{II})}} &= w^{(\mathrm{III})}\big|_{z=0.5h^{(\mathrm{II})}}, \end{aligned} \tag{4}$$

$$\begin{aligned} q_z^{(\mathrm{I})}\big|_{z=-0.5h^{(II)}} &= q_z^{(II)}\big|_{z=-0.5h^{(II)}}, \\ q_z^{(\mathrm{II})}\big|_{z=0.5h^{(II)}} &= q_z^{(III)}\big|_{z=0.5h^{(II)}}. \end{aligned} \tag{5}$$

Based on nonlocal thermo-viscoelasticity model (Li et al. 2021a), the basic equations for one-dimensional nonlocal thermo-viscoelastic problem of layer-by-layer viscoelastic sandwich nanoplates can be formulated as follows (in the absence of body force and internal heat generation):

(i). Motion equation:

$$\frac{\partial \sigma_{zz}^{(i)}}{\partial z^2} = \rho^{(i)} \frac{\partial^2 w^{(i)}}{\partial t^2} \tag{6}$$

(ii). Strain–displacement relation:

$$\varepsilon_{zz}^{(i)} = \frac{\partial w^{(i)}}{\partial z} \tag{7}$$

(iii). Energy equation:

$$\frac{\partial q_z^{(i)}}{\partial z} + \rho^{(i)} T_0 \frac{\partial S^{(i)}}{\partial t} = 0 \tag{8}$$

(iv). Nonlocal heat conduction equation:

$$\left[1 - \left(\chi_q^{(i)}\right)^2 \frac{\partial^2}{\partial x^2}\right] q_z^{(i)} = -\kappa^{(i)} \frac{\partial \theta^{(i)}}{\partial z} \tag{9}$$

(v). Constitutive equations:

$$\left[1 - (e_0 a)_{(i)}^2 \frac{\partial^2}{\partial z^2}\right] \sigma_{zz}^{(i)} = \left(\frac{2}{3} R^{(i)} + K_0^{(i)}\right) \frac{\partial w^{(i)}}{\partial z} - \gamma^{(i)} \theta^{(i)} \tag{10}$$

$$\left[1-(e_0a)_{(i)}^2\frac{\partial^2}{\partial z^2}\right]\sigma_{yy}^{(i)}=\left[1-(e_0a)_{(i)}^2\frac{\partial^2}{\partial z^2}\right]\sigma_{xx}^{(i)}=\left(-\frac{1}{2}R^{(i)}+K_0^{(i)}\right)\frac{\partial w^{(i)}}{\partial z}-\gamma^{(i)}\theta^{(i)} \tag{11}$$

$$\sigma_{xy}^{(i)}=\sigma_{yz}^{(i)}=\sigma_{zx}^{(i)}=0 \tag{12}$$

$$\rho^{(i)}S^{(i)}=\gamma^{(i)}\varepsilon_{zz}^{(i)}+\frac{\rho^{(i)}c_E^{(i)}}{T_0}\theta^{(i)} \tag{13}$$

where

$$R^{(i)}=2\mu^{(i)}\left[1-(A^*)^{(i)}\int_0^t \mathrm{e}^{-(\beta^*)^{(i)}}t^{(\alpha^*)^{(i)}-1}\mathrm{d}t\right],\quad R^{(i)}(0)=2\mu^{(i)},$$

$$K_0^{(i)}=\lambda^{(i)}+\frac{2}{3}\mu^{(i)},\quad \gamma^{(i)}=\left(3\lambda^{(i)}+2\mu^{(i)}\right)\alpha_T^{(i)},$$

$$0<(\alpha^*)^{(i)}<1,\quad (\beta^*)^{(i)}>0,\quad 0\le(A^*)^{(i)}<\frac{(\beta^*)^{(i)}}{\Gamma\left[(\alpha^*)^{(i)}\right]},$$

in which $(\alpha^*)^{(i)}$, $(\beta^*)^{(i)}$ and $(A^*)^{(i)}$ represent dimensionless empirical constants. In addition, relaxation function $R^{(i)}$ satisfies the conditions: $R^{(i)}>0$, $\frac{\mathrm{d}}{\mathrm{d}t}R^{(i)}<0$. The superscript/subscript i represents the material constants and variable considered in the Medium I, II, III of the viscoelastic laminated sandwich nanoplates. In the constitutive Eqs. (10) and (11), the elastic nonlocal parameter e_0a has been used to evaluate size effect of elastic deformation in the analysis of size-dependent buckling, bending and vibration of nanobeam (Reddy 2007). Within theoretical formulation of Eringen's nonlocal elasticity model, the material constant e_0a/l refers to the long-range forces between atoms, where e_0 is a material dependent constant, a is internal characteristic length (e.g., lattice spacing between individual atoms, granular size, etc.), l is external characteristic length (e.g., crack length, wave length, etc.). Eringen (1983) suggested that the parameter e_0 is a constant appropriated to the materials and structures at the nanoscale, for example $e_0=0.39$. However, Eringen (1983) also pointed out that the value of e_0 should be determined by experimentations or matched through dispersion curves of plane waves with those of atomic lattice dynamics. So far, the issue is still not thoroughly solved and deserves more investigation efforts on this topic. More importantly, some scholars believed that the parameter e_0 should be valued as a magnitude that depends on the order of hundreds or even thousands, so that the size effect of elastic deformation to have significance. Additionally, it has been found that the parameter a can be valued as the length of a C–C bond (i.e., $a=1.42\times10^{-8}$cm) for a single walled carbon nanotube (Lu 1997). In view of current studies, one can conclude that the parameter e_0a is always arbitrarily chosen to predict the elastic nonlocal effect on structural dynamic responses of nanoplate or nanocomposites in different material systems (Yu et al. 2016; Li et al. 2019b, 2021). However, the determination of its true value is still far from a common agreement in the field of nano-mechanics. The term $\left(\chi_q^{(i)}\right)^2\frac{\partial^2 q_z^{(i)}}{\partial x^2}$ represents the size effect of heat transfer. In general, classical Fourier heat conduction law is only valid in the cases of $l<<h$ and $\tau_q<<t_0$, where l is the mean free path, h is the characteristic length of the system, τ_q is the thermal relaxation time, t_0 is the characteristic time of the heat transport process under consideration. However, this phenomenological law will questionable if $\tau_q<<t_0$, $l\to h$, and the size effect of heat transfer should be seriously considered. To author's knowledge, the mathematical term $\left(\chi_q^{(i)}\right)^2\frac{\partial^2 q_z^{(i)}}{\partial x^2}$ has been used to predict thermal nonlocal effect in size-dependent thermo-mechanical problems of bi-layered elastic nanocomposites (Yu et al. 2016), multilayered piezoelectric nanoplates (Li et al. 2019b), and bi-layered composite viscoelastic nanoplate (Li et al. 2021a).

Substitution of Eqs. (7) and (10) into Eq. (6) yields the governing equation of motion:

$$\left(\frac{2}{3}R^{(i)}+K_0^{(i)}\right)\frac{\partial^2 w^{(i)}}{\partial z^2}-\gamma^{(i)}\frac{\partial\theta^{(i)}}{\partial z}=\rho^{(i)}\left[1-(e_0a)_{(i)}^2\frac{\partial^2}{\partial z^2}\right]\frac{\partial^2 w^{(i)}}{\partial t^2}. \tag{14}$$

Substitution of Eqs. (7), (9) and (13) into Eq. (8) yields the governing equation of temperature:

$$\kappa^{(i)}\frac{\partial^2\theta^{(i)}}{\partial z^2}=\left[1-\left(\chi_q^{(i)}\right)^2\frac{\partial^2}{\partial z^2}\right]\left[T_0\gamma^{(i)}\frac{\partial^2 w^{(i)}}{\partial z\partial t}+\rho^{(i)}c_E^{(i)}\frac{\partial\theta^{(i)}}{\partial t}\right]. \tag{15}$$

For convenience, the dimensionless quantities are introduced as follows:

$$\left[\bar{z},\bar{w}^{(i)},(\bar{e}_0\bar{a})^{(i)},\bar{\chi}_q^{(i)}\right]=c\eta\left[z,w^{(i)},(e_0a)^{(i)},\chi_q^{(i)}\right],\quad \bar{t}=c^2\eta t,$$
$$\left(\bar{\sigma}_{xx}^{(i)},\bar{\sigma}_{yy}^{(i)},\bar{\sigma}_{zz}^{(i)}\right)=\frac{1}{K_0^{(\mathrm{I})}}\left(\sigma_{xx}^{(i)},\sigma_{yy}^{(i)},\sigma_{zz}^{(i)}\right),\quad \bar{\theta}^{(i)}=\frac{\theta^{(i)}}{T_0},\quad \bar{R}^{(i)}=\frac{2}{3K_0^{(\mathrm{I})}}R^{(i)},$$
$$\bar{q}_z^{(i)}=\frac{q_z^{(i)}}{\kappa^{(\mathrm{I})}T_0c\eta},\quad \eta=\frac{\rho^{(\mathrm{I})}c_E^{(\mathrm{I})}}{\kappa^{(\mathrm{I})}},\quad c^2=\frac{K_0^{(\mathrm{I})}}{\rho^{(\mathrm{I})}}. \tag{16}$$

In terms of Eqs. (10), (11), (14) and (15) can be further written as:

$$\left[1-(\bar{e}_0\bar{a})^2_{(i)}\frac{\partial^2}{\partial\bar{z}^2}\right]\bar{\sigma}^{(i)}_{zz}=\left(\bar{R}^{(i)}+\frac{K_0^{(i)}}{K_0^{(\mathrm{I})}}\right)\frac{\partial\overline{w}^{(i)}}{\partial\bar{z}}-\varphi^{(i)}\overline{\theta}^{(i)}, \tag{17}$$

$$\begin{aligned}\left[1-(\bar{e}_0\bar{a})^2_{(i)}\frac{\partial^2}{\partial\bar{z}^2}\right]\bar{\sigma}^{(i)}_{yy}&=\left[1-(\bar{e}_0\bar{a})^2_{(i)}\frac{\partial^2}{\partial\bar{z}^2}\right]\bar{\sigma}^{(i)}_{xx}\\&=\left(-\frac{1}{2}\bar{R}^{(i)}+\frac{K_0^{(i)}}{K_0^{(\mathrm{I})}}\right)\frac{\partial\overline{w}^{(i)}}{\partial\bar{z}}-\varphi^{(i)}\overline{\theta}^{(i)},\end{aligned} \tag{18}$$

$$\psi^{(i)}\frac{\partial^2\overline{w}^{(i)}}{\partial\bar{z}^2}-\phi^{(i)}\frac{\partial\overline{\theta}^{(i)}}{\partial\bar{z}}=\left[1-(\bar{e}_0\bar{a})^2_{(i)}\frac{\partial^2}{\partial\bar{z}^2}\right]\frac{\partial^2\overline{w}^{(i)}}{\partial\bar{t}^2}, \tag{19}$$

$$\frac{\partial^2\overline{\theta}^{(i)}}{\partial\bar{z}^2}=\left[1-\left(\chi_q^{(i)}\right)^2\frac{\partial^2}{\partial\bar{z}^2}\right]\left(g^{(i)}\frac{\partial^2\overline{w}^{(i)}}{\partial\bar{z}\partial\bar{t}}+f^{(i)}\frac{\partial\overline{\theta}^{(i)}}{\partial\bar{t}}\right), \tag{20}$$

where

$$\varphi^{(i)}=\frac{\gamma^{(i)}T_0}{K_0^{(i)}},\quad \psi^{(i)}=\frac{K_0^{(\mathrm{I})}}{\rho^{(i)}c^2}\left(\bar{R}^{(i)}+\frac{K_0^{(i)}}{K_0^{(\mathrm{I})}}\right),$$
$$\phi^{(i)}=\frac{\gamma^{(i)}T_0}{\rho^{(i)}c^2},\quad g^{(i)}=\frac{\gamma^{(i)}}{\kappa^{(i)}\eta_1},\quad f^{(i)}=\frac{\rho^{(i)}c_E^{(i)}}{\kappa^{(i)}\eta}.$$

3 Analytical solutions

Performing Laplace transformation:

$$f'(s)=L[f(t)]=\int_0^\infty e^{-st}f(t)\mathrm{d}t, \tag{21}$$

to both sides of Eqs. (17) to (20) with zero initial condition (2) yields:

$$\left[1-(\bar{e}_0\bar{a})^2_{(i)}\frac{d^2}{d\bar{z}^2}\right]\bar{\sigma}'^{(i)}_{zz}=\left[\bar{R}'^{(i)}(s)+\frac{K_0^{(i)}}{K_0^{\mathrm{I}}}\right]\frac{d\bar{w}'^{(i)}(\bar{z},s)}{d\bar{z}}-\varphi^{(i)}\bar{\theta}'^{(i)}, \tag{22}$$

$$\begin{aligned}\left[1-(\bar{e}_0\bar{a})^2_{(i)}\frac{d^2}{d\bar{z}^2}\right]\bar{\sigma}'^{(i)}_{yy}&=\left[1-(\bar{e}_0\bar{a})^2_{(i)}\frac{d^2}{d\bar{z}^2}\right]\bar{\sigma}'^{(i)}_{xx}\\&=\left(-\frac{1}{2}\bar{R}'^{(i)}+\frac{K_0^{(i)}}{K_0^{(\mathrm{I})}}\right)\frac{d\bar{w}'^{(i)}}{d\bar{z}}\\&\quad-\varphi^{(i)}\bar{\theta}'^{(i)},\end{aligned} \tag{23}$$

$$\psi^{(i)}\frac{\mathrm{d}^2\overline{w}'^{(i)}}{\mathrm{d}\bar{z}^2}-\phi^{(i)}\frac{\mathrm{d}\overline{\theta}'^{(i)}}{\mathrm{d}\bar{z}}=s^2\left[1-(\bar{e}_0\bar{a})^2_{(i)}\frac{\mathrm{d}^2}{\mathrm{d}\bar{z}^2}\right]\overline{w}'^{(i)}, \tag{24}$$

$$\frac{\mathrm{d}^2\bar{\theta}'^{(i)}}{\mathrm{d}\bar{z}^2}=s\left[1-\left(\chi_q^{(i)}\right)^2\frac{\mathrm{d}^2}{\mathrm{d}\bar{z}^2}\right]\left(1-\bar{\chi}^2_{(i)}\frac{\mathrm{d}^2}{\mathrm{d}\bar{z}^2}\right)\left(g^{(i)}\frac{\mathrm{d}\bar{w}'^{(i)}}{\mathrm{d}\bar{z}}+f^{(i)}\bar{\theta}'^{(i)}\right), \tag{25}$$

where

$$\bar{R}'^{(i)}=\frac{4\mu^{(i)}}{3sK_0^{(i)}}\left\{1-(A^*)^{(i)}\Gamma\left[(\alpha^*)^{(i)}\right]\Big/\left[s+(\beta^*)^{(i)}\right]^{(\alpha^*)^{(i)}}\right\}.$$

In terms of dimensionless quantities (16), boundary conditions and interfacial conditions in the Laplace transformation domain are given as below:

$$\bar{\sigma}'^{(\mathrm{I})}_{zz}\left(\pm h^{(\mathrm{I})},s\right)=0,\quad \bar{\theta}'^{(\mathrm{I})}\left(\pm h^{(\mathrm{I})},s\right)=f(s), \tag{26}$$

$$\begin{aligned}&\overline{w}'^{(\mathrm{I})}\Big|_{\bar{z}=-0.5\bar{h}^{(\mathrm{II})}}=\overline{w}'^{(\mathrm{II})}\Big|_{\bar{z}=-0.5\bar{h}^{(\mathrm{II})}},\\&\overline{w}'^{(\mathrm{II})}\Big|_{\bar{z}=0.5\bar{h}^{(\mathrm{II})}}=\overline{w}'^{(\mathrm{III})}\Big|_{\bar{z}=0.5\bar{h}^{(\mathrm{II})}},\end{aligned} \tag{27}$$

$$\begin{aligned}&\bar{q}'^{(\mathrm{I})}_z\Big|_{\bar{z}=-0.5\bar{h}^{(\mathrm{II})}}=\bar{q}'^{(\mathrm{II})}_z\Big|_{\bar{z}=-0.5\bar{h}^{(\mathrm{II})}},\\&\bar{q}'^{(\mathrm{II})}_z\Big|_{\bar{z}=0.5\bar{h}^{(\mathrm{II})}}=\bar{q}'^{(\mathrm{III})}_z\Big|_{\bar{z}=0.5\bar{h}^{(\mathrm{II})}}.\end{aligned} \tag{28}$$

Eliminating $\bar{\theta}'^{(i)}$ between Eqs. (24) and (25), the following fourth-order ordinary differential equation is derived:

$$\frac{\mathrm{d}^4\bar{w}'^{(i)}}{\mathrm{d}\bar{z}^4}-p^{(i)}\frac{\mathrm{d}^2\bar{w}'^{(i)}}{\mathrm{d}\bar{z}^2}+r^{(i)}\overline{w}'^{(i)}=0, \tag{29}$$

where

$$p^{(i)}=\frac{s\phi^{(i)}g^{(i)}+sf^{(i)}\left[\psi^{(i)}+s^2(\bar{e}_0\bar{a})^2_{(i)}\right]+s^2\left(1+sf^{(i)}\bar{\chi}^2_{(i)}\right)}{s\phi^{(i)}g^{(i)}\bar{\chi}^2_{(i)}+\left[1+sf^{(i)}\left(\chi_q^{(i)}\right)^2\right]\left[\psi^{(i)}+s^2(\bar{e}_0\bar{a})^2_{(i)}\right]},$$

Table 1 Material parameters of Medium I (Polymethyl Methacrylate)

$\lambda^{(\mathrm{I})}=453.7\times10^7\mathrm{kg/m\,s^2}$	$\mu^{(\mathrm{I})}=194\times10^7\mathrm{kg/m\,s^2}$	$\rho^{(\mathrm{I})}=1.2\times10^3\mathrm{kg/m^3}$
$\kappa^{(\mathrm{I})}=0.55\mathrm{W/(m\,K)}$	$E^{(\mathrm{I})}=525\times10^7\mathrm{N/m^2}$	$\gamma^{(\mathrm{I})}=210\times10^4\mathrm{N/m^2K}$
$\alpha_T^{(\mathrm{I})}=13\times10^{-5}\mathrm{K^{-1}}$	$c_E^{(\mathrm{I})}=1.4\times10^3\mathrm{J/(kg\,K)}$	$T_0=293$ K
$c_1=2200\mathrm{m/s}$		

$$r^{(i)} = \frac{s^3 f^{(i)}}{s\phi^{(i)} g^{(i)} \overline{\chi}_{(i)}^2 + \left[1 + sf^{(i)}\left(\chi_q^{(i)}\right)^2\right]\left[\psi^{(i)} + s^2(\overline{e}_0\overline{a})_{(i)}^2\right]}.$$

In a similar manner, $\overline{\theta}'^{(i)}$ satisfies the ordinary differential equation:

$$\frac{d^4\overline{\theta}'^{(i)}}{d\overline{z}^4} - p^{(i)}\frac{d^2\overline{\theta}'^{(i)}}{d\overline{z}^2} + r^{(i)}\overline{\theta}'^{(i)} = 0. \tag{30}$$

In view of Eqs. (29) and (30), the solutions of displacement and temperature are given as below:

$$\overline{w}'^{(i)}(\overline{z},\ s) = \sum_{j=1}^{4} \overline{w}_j^{(i)} e^{-k_j^{(N)}\overline{z}}, \quad \overline{\theta}'^{(i)}(\overline{z},\ s) = \sum_{j=1}^{4} \overline{\theta}_j^{(i)} e^{-k_j^{(i)}\overline{z}}, \tag{31}$$

where $\overline{w}_j^{(i)}$ and $\overline{\theta}_j^{(i)}$ are parameters depending only on s. The roots with positive real parts $k_j^{(i)}(j = 1, 2, 3, 4)$ satisfy the following characteristic equation:

$$\left(k_j^{(i)}\right)^4 - p^{(i)}\left(k_j^{(i)}\right)^2 + r^{(i)} = 0, \tag{32}$$

where

$$k_1^{(i)} = \sqrt{\frac{p^{(i)} + \sqrt{\left(p^{(i)}\right)^2 - 4r^{(i)}}}{2}}, \quad k_2^{(i)} = -\sqrt{\frac{p^{(i)} + \sqrt{\left(p^{(i)}\right)^2 - 4r^{(i)}}}{2}},$$

$$k_3^{(i)} = \sqrt{\frac{p^{(i)} - \sqrt{\left(p^{(i)}\right)^2 - 4r^{(i)}}}{2}}, \quad k_4^{(i)} = -\sqrt{\frac{p^{(i)} - \sqrt{\left(p^{(i)}\right)^2 - 4r^{(i)}}}{2}}.$$

Substitution of Eq. (31) into Eq. (24) yields:

$$\overline{\theta}'^{(i)}(\overline{z},\ s) = \sum_{j=1}^{4} \overline{\theta}_j^{(i)} e^{-k_j^{(i)}\overline{z}} = \sum_{j=1}^{4} \delta_j^{(i)} \overline{w}_j^{(i)} e^{-k_j^{(i)}\overline{z}} \tag{33}$$

where

$$\delta_j^{(i)} = -\frac{\left[\psi^{(i)} + (\overline{e}_0\overline{a})_{(i)}^2 s^2\right]\left(k_j^{(i)}\right)^2 - s^2}{k_j^{(i)}\phi^{(i)}}.$$

Substitution the solutions of displacement and temperature into the constitutive equations of (22) and (23) yields:

$$\overline{\sigma}'^{(i)}_{zz}(\overline{z},\ s) = \sum_{j=1}^{4} \chi_{1j}^{(i)} \overline{w}_j^{(i)} e^{-k_j^{(i)}\overline{z}},$$
$$\overline{\sigma}'^{(i)}_{yy}(\overline{z},\ s) = \overline{\sigma}'^{(i)}_{xx}(\overline{z},\ s) = \sum_{j=1}^{4} \chi_{2j}^{(i)} \overline{w}_j^{(i)} e^{-k_j^{(i)}\overline{z}}, \tag{34}$$

where

$$\chi_{2j}^{(i)} = \frac{-\left(k_j^{(i)}\right)^2\left[\phi^{(i)}\overline{R}'^{(i)}(s) + \phi^{(i)}\frac{K_0^{(i)}}{K_0^{(\mathrm{I})}} - \varphi^{(i)} l^{(i)}\right] - s^2\varphi^{(i)}\left[1 - (\overline{e}_0\overline{a})_{(i)}^2\left(k_j^{(i)}\right)^2\right]}{\phi^{(i)} k_j^{(i)}\left[1 - (\overline{e}_0\overline{a})_{(i)}^2\left(k_j^{(i)}\right)^2\right]}.$$

By introducing solutions of stress and temperature into the boundary conditions (26), and then one has:

$$\sum_{j=1}^{4} \chi_{1j}^{(\mathrm{I})} \overline{w}_j^{(\mathrm{I})} e^{k_j(\mathrm{I})h^{(\mathrm{I})}} = 0, \quad \sum_{j=1}^{4} \chi_{1j}^{(\mathrm{I})} \overline{w}_j^{(\mathrm{I})} e^{-k_j(\mathrm{I})h^{(\mathrm{I})}} = 0, \tag{35}$$

$$\sum_{j=1}^{4} \delta_j^{(\mathrm{I})} \overline{w}_j^{(\mathrm{I})} e^{k_j(\mathrm{I})h^{(\mathrm{I})}} = 1/s, \quad \sum_{j=1}^{4} \delta_j^{(\mathrm{I})} \overline{w}_j^{(\mathrm{I})} e^{-k_j(\mathrm{I})h^{(\mathrm{I})}} = f(s). \tag{36}$$

Clearly, the unknown parameters $\overline{w}_j^{(\mathrm{I})}$ can be obtained by dealing with linear algebraic equations of (35) and (36). To acquire the analytical formula of $\overline{w}_j^{(\mathrm{II})}$, the interfacial conditions at $\overline{z} = \pm 0.5\overline{h}^{(\mathrm{II})}$ [i.e. Eqs. (27) and (28)] are adopted. According to the dimensionless quantities (16), the nonlocal heat conduction Eq. (9) for Medium I and II in the Laplace transformation domain are:

$$\left[1 - \left(\chi_q^{(\mathrm{I})}\right)^2\frac{d^2}{dz^2}\right]\overline{q}_z'^{(\mathrm{I})}\big|_{\overline{z}=-0.5\overline{h}^{(\mathrm{II})}} = -\frac{d\overline{\theta}'^{(\mathrm{I})}}{d\overline{z}}\big|_{\overline{z}=-0.5\overline{h}^{(\mathrm{II})}}, \tag{37}$$

$$\left[1 - \left(\chi_q^{(\mathrm{II})}\right)^2\frac{d^2}{dz^2}\right]\overline{q}_z'^{(\mathrm{II})}\big|_{\overline{z}=0.5\overline{h}^{(\mathrm{II})}} = -\varsigma\frac{d\overline{\theta}^{(\mathrm{II})}}{d\overline{z}}\big|_{\overline{z}=0.5\overline{h}^{(\mathrm{II})}}, \tag{38}$$

where $\varsigma = \kappa^{(\mathrm{II})}\kappa^{(\mathrm{II})}\kappa^{(\mathrm{I})} - \kappa^{(\mathrm{I})}$. From Eqs. (37) and (38), the heat flux between the two adjacent layers at the interface $z = \pm h^{(\mathrm{II})}$ in the Laplace transformation domain are given as below:

$$q_z^{(\mathrm{I})}\big|_{z=-0.5h^{(\mathrm{II})}} = \frac{1}{1 - \left(\chi_q^{(\mathrm{I})}\right)^2\left(k_j^{(\mathrm{I})}\right)^2}\sum_{j=1}^{4} k_j^{(\mathrm{I})}\delta_j^{(\mathrm{I})}\overline{w}_j^{(\mathrm{I})} e^{0.5k_j(\mathrm{I})\overline{h}^{(\mathrm{II})}}, \tag{39}$$

$$q_z^{(\mathrm{II})}\big|_{z=0.5h^{(\mathrm{II})}} = \frac{1}{1 - \left(\chi_q^{(\mathrm{II})}\right)^2\left(k_j^{(\mathrm{II})}\right)^2}\sum_{j=1}^{4} k_j^{(\mathrm{II})}\delta_j^{(\mathrm{II})}\overline{w}_j^{(\mathrm{II})} e^{-0.5k_j(\mathrm{II})\overline{h}^{(\mathrm{II})}}. \tag{40}$$

Substitution the solutions of displacement and temperature into Eqs. (27) and (28) yields:

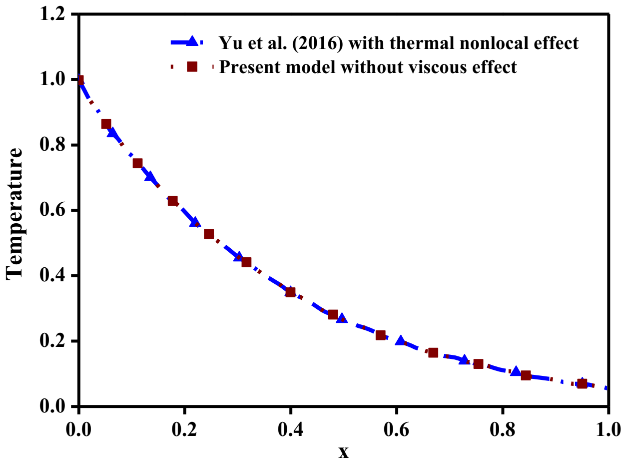

Fig. 2 Comparison studies of present model without piezoelectric effect and Yu et al. (2016)

$$\sum_{j=1}^{4}\overline{w}_j^{(\mathrm{I})}\mathrm{e}^{0.5k_j(\mathrm{I})\overline{h}^{(\mathrm{II})}}-\sum_{j=1}^{4}\overline{w}_j^{(\mathrm{II})}\mathrm{e}^{0.5k_j(\mathrm{II})\overline{h}^{(\mathrm{II})}}=0, \tag{41}$$

$$\sum_{j=1}^{4}\overline{w}_j^{(\mathrm{II})}\mathrm{e}^{-0.5k_j(\mathrm{II})\overline{h}^{(\mathrm{II})}}-\sum_{j=1}^{4}\overline{w}_j^{(\mathrm{I})}\mathrm{e}^{-0.5k_j(\mathrm{I})\overline{h}^{(\mathrm{II})}}=0, \tag{42}$$

$$\begin{aligned}&\frac{1}{1-\left(\chi_q^{(\mathrm{I})}\right)^2\left(k_j^{(\mathrm{I})}\right)^2}\sum_{j=1}^{4}k_j^{(\mathrm{I})}\delta_j^{(\mathrm{I})}\overline{w}_j^{(\mathrm{I})}\mathrm{e}^{k_j(\mathrm{I})\overline{h}^{(\mathrm{I})}}\\&-\frac{\kappa^{(\mathrm{II})}}{\kappa^{(\mathrm{I})}}\frac{1}{1-\left(\chi_q^{(\mathrm{II})}\right)^2\left(k_j^{(\mathrm{II})}\right)^2}\sum_{j=1}^{4}k_j^{(\mathrm{II})}\delta_j^{(\mathrm{II})}\overline{w}_j^{(\mathrm{II})}\mathrm{e}^{k_j(\mathrm{II})\overline{h}^{(\mathrm{II})}}\\&=0,\end{aligned} \tag{43}$$

$$\begin{aligned}&\frac{\kappa_{11}^{(\mathrm{II})}}{\kappa_{11}^{(\mathrm{I})}}\frac{1}{1-\left(\chi_q^{(\mathrm{II})}\right)^2\left(k_j^{(\mathrm{II})}\right)^2}\sum_{j=1}^{4}k_j^{(\mathrm{II})}\delta_j^{(\mathrm{II})}\overline{w}_j^{(\mathrm{II})}\mathrm{e}^{-k_j(\mathrm{II})\overline{h}^{(\mathrm{II})}}\\&-\frac{1}{1-\overline{\chi}_{(\mathrm{I})}^2\left(k_j^{(\mathrm{I})}\right)^2}\sum_{j=1}^{4}k_j^{(\mathrm{I})}\delta_j^{(\mathrm{I})}\overline{w}_j^{(\mathrm{I})}\mathrm{e}^{-k_j(\mathrm{I})\overline{h}^{(\mathrm{I})}}\\&=0.\end{aligned} \tag{44}$$

The analytical formula of $\overline{w}_j^{(\mathrm{II})}$ can be obtained by solving the linear algebraic equations (41) to (44). Thus far, the solutions of the problem formulated in Sect. 2 are totally completed in the Laplace transformation domain.

4 Results and discussion

In this section, a numerical inverse Laplace transformation (NILT) based on fast Fourier transformation (Brancik 1999) will be applied to achieve the structural thermo-viscoelastic responses in time domain. The dimensionless results of temperature, displacement, and compressive stress are graphically illustrated. The influences of nonlocal parameter and material constants ratios on structural dynamic responses will be evaluated and discussed by the method of controlling variables. The viscoelastic material constants of Medium II are valued by ratios of those in Medium I (III), whose material constants can refer to Table 1. In addition, it needs to be emphasized that the non-mentioned material parameters of Medium I (III) are the same as those in Medium II unless the specific illustration attached.

Figures 3, 4, 5, 6, 7, 8, 9 present the dimensionless responses along the dimensionless thickness of the sandwich nanoplates for dimensionless time $t = 0.2$. The dimensionless thickness of the layer-by-layer viscoelastic sandwich nanoplate $h^{(I)}(h^{(\mathrm{III})})$ and $h^{(\mathrm{II})}$ are respectively valued as 0.50 and 1.00. In addition, the symmetric thermal shock loadings at the bounding planes $z = h^{(\mathrm{I})}$ and $z = h^{(\mathrm{III})}$ will adopt the form as $f(t) = 25t^2$. As a consequence, the temperature rise at $z = h^{(\mathrm{I})}$ and $z = h^{(\mathrm{III})}$ is 1.0. Clearly, the analytical model formulated in Sect. 2 will be reduced to a one layer with one end subjected to time-dependent thermal loads if the following conditions are satisfied: (i) the viscous effect is ignored; (ii) temperature change at the lower surface is assumed to be zero. As shown in Fig. 2, the predicted results of temperature response match well with that in Yu et al. (2016). This ensures the validity and accuracy of the numerical algorithm via Laplace transformation adopted in this work.

4.1 The effect of thermal nonlocal parameter $\overline{\chi}_q^{(i)}$

The effect of nonlocal parameter $\overline{\chi}_q^{(i)}$ on the structural responses is mainly discussed in this subsection. During the analysis, the size effect of elastic deformation is neglected, i.e. $\overline{e}_0\overline{a}^{(i)} = 0$. As shown in Fig. 3, the dimensionless results for $\overline{\chi}_q^{(\mathrm{I})} = \overline{\chi}_q^{(\mathrm{II})} = \overline{\chi}_q^{(\mathrm{III})} = \overline{\chi}_q^{(i)}$ are graphically illustrated. If $\overline{\chi}_q^{(i)}$ increases, the following conclusions will be reached. Firstly, the absolute values of temperature and compressive stress are greatly enhanced, even at the interfaces. Secondly, the displacement will become smoother, whilst the Medium II deforms larger and a clear increase of displacement is observed at the interfaces. Figure 4 presents dimensionless results for $\overline{\chi}_q^{(\mathrm{I})}\left(\overline{\chi}_q^{(\mathrm{III})}\right) \neq \overline{\chi}_q^{(\mathrm{II})}$. If $\overline{\chi}_q^{(\mathrm{I})}\left(\overline{\chi}_q^{(\mathrm{III})}\right)$ is larger than that in Medium II (i.e.)$\overline{\chi}_q^{(\mathrm{I})}\big/\overline{\chi}_q^{(\mathrm{II})} > 1.00$, it is observed that: (i) the temperature is larger in Medium I and III, but lower in Medium II; (ii) the displacement is almost unchanged in Medium I and III, while Medium II deforms smaller; (iii) the comprehensive stresses $\overline{\sigma}'_{zz}$ and $\overline{\sigma}'_{xx}$ ($\overline{\sigma}'_{yy}$) increase in Medium I and III, but reduced in Medium II; (iv) an

Fig. 3 Dimensionless results for $\overline{\chi}_q^{(\mathrm{I})} = \overline{\chi}_q^{(\mathrm{II})} = \overline{\chi}_q^{(\mathrm{III})} = \overline{\chi}_q^{(i)}$

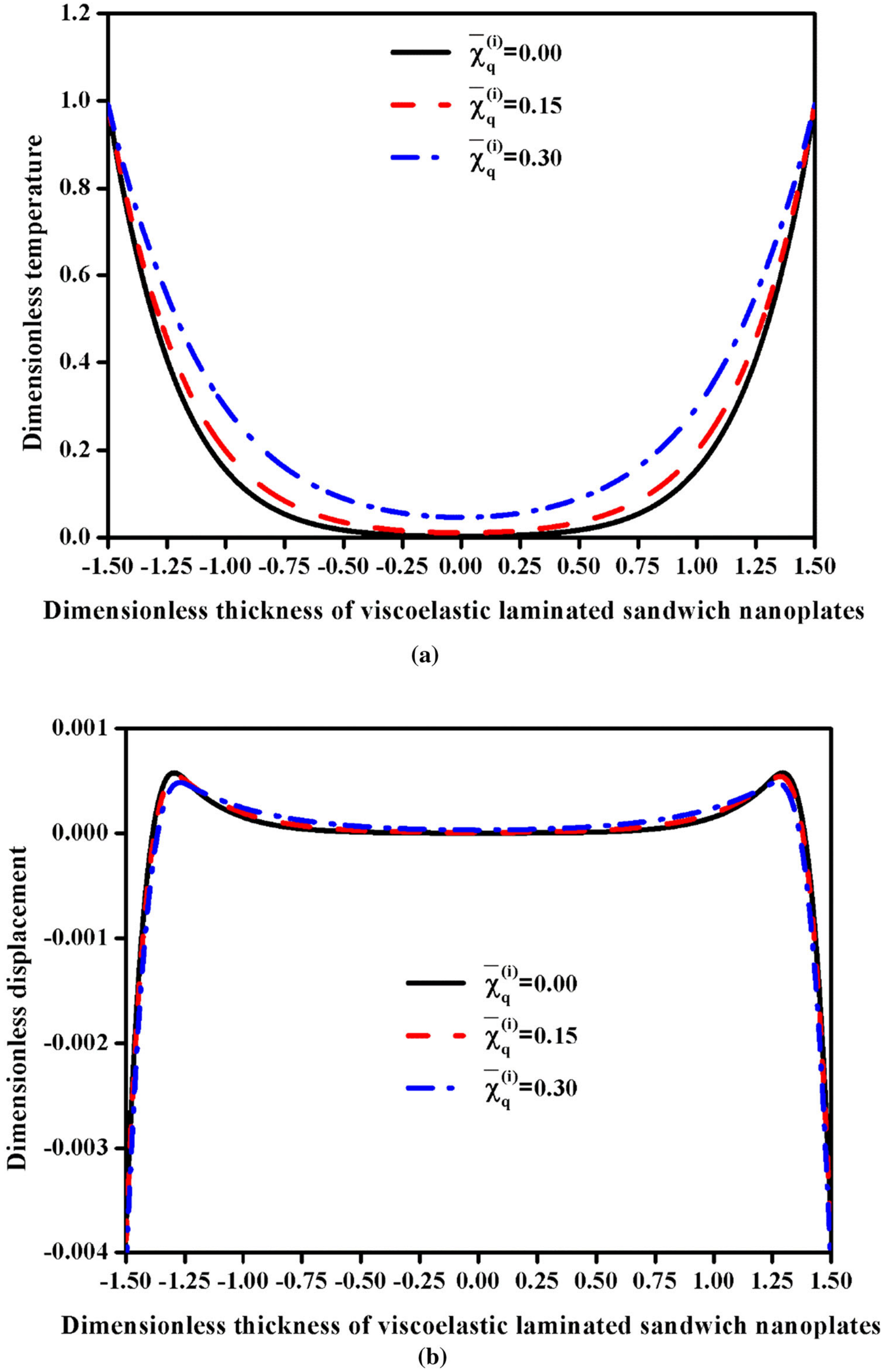

evident jump of dynamic responses exists at the interfaces, that is, the temperature, displacement or compressive stress $\bar{\sigma}'_{zz}$ ($\bar{\sigma}'_{yy}$) will suddenly jumps from a higher value to a lower one. If the ratio $\overline{\chi}_q^{(\mathrm{I})} \big/ \overline{\chi}_q^{(\mathrm{II})} < 1.00$ is adopted, it is obtained that: (i) temperature response is not changed in both Medium I and III, but it will be greatly increased in Medium II; (ii) the Medium II deforms larger, but there is no change for the deformation in Medium I and III; (iii) the comprehensive stresses $\bar{\sigma}'_{zz}$ and $\bar{\sigma}'_{xx}$ ($\bar{\sigma}'_{yy}$) is significantly

Fig. 3 continued

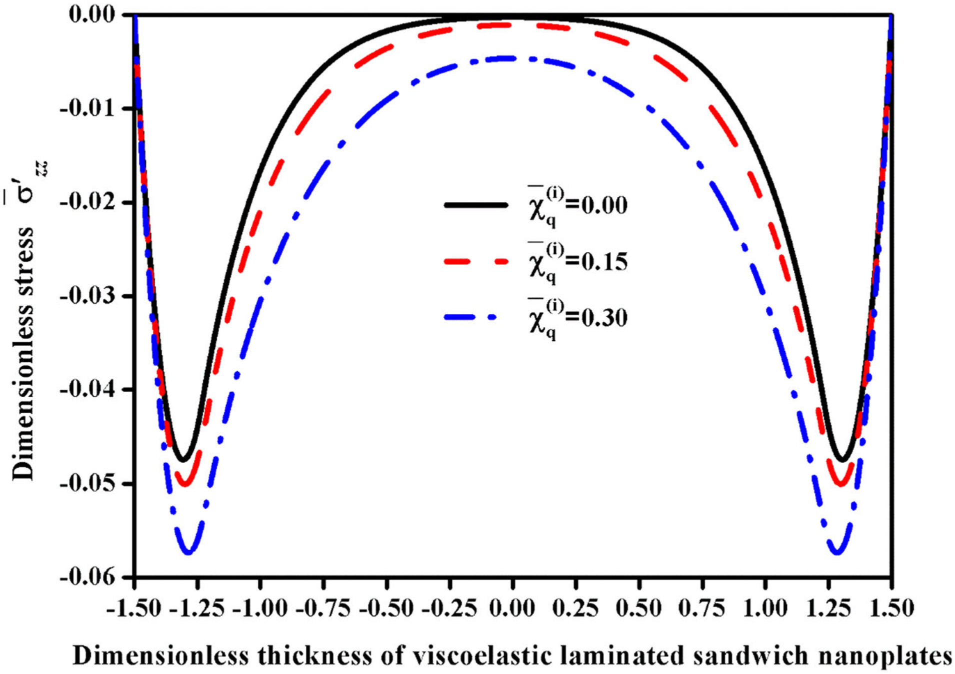

(c)

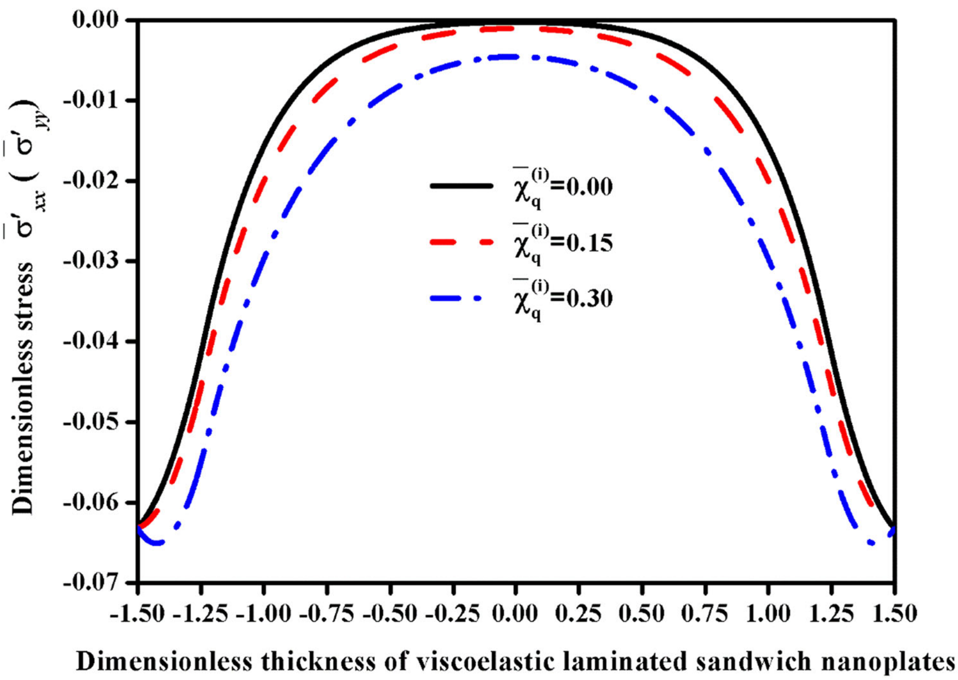

(d)

improved in Medium II, but almost unchanged in both Medium I and III; (iv) the responses of temperature, displacement or compressive stress abruptly jump to a higher value at the interfaces. It is known that the surface coating at the two adjacent layers of the viscoelastic nanoplates is always designed to avoid larger heat energy and thermal induced stresses at the interfaces. This is very important for the safe working of viscoelastic laminated sandwich nanocomposites subjected to time-varying symmetric thermal shock loadings. From Figs. 3 and 4, it is clear that

Fig. 4 Dimensionless results for different combinations of $\overline{\chi}_q^{(i)}$

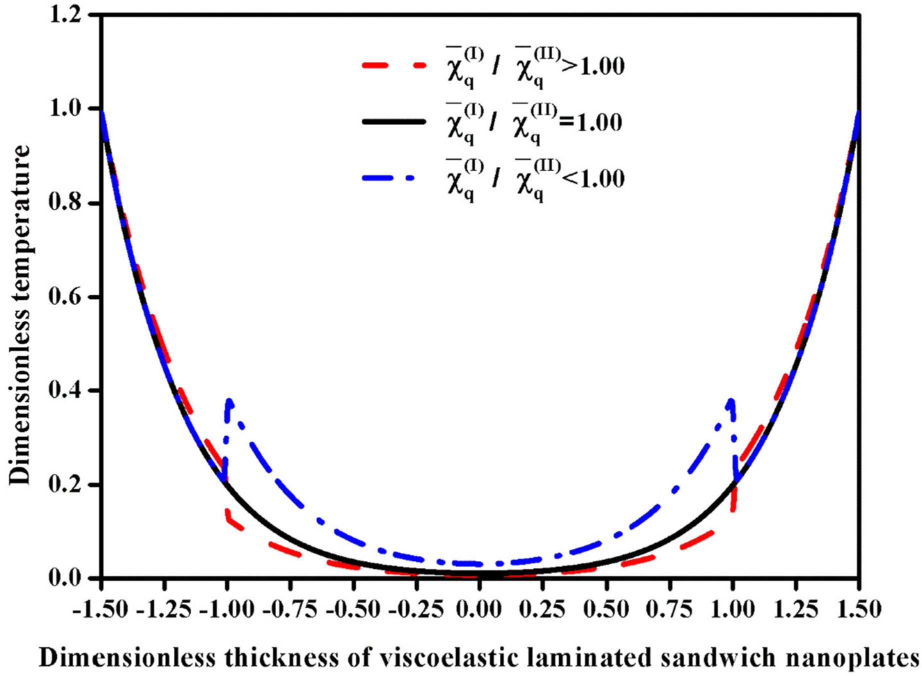

(a)

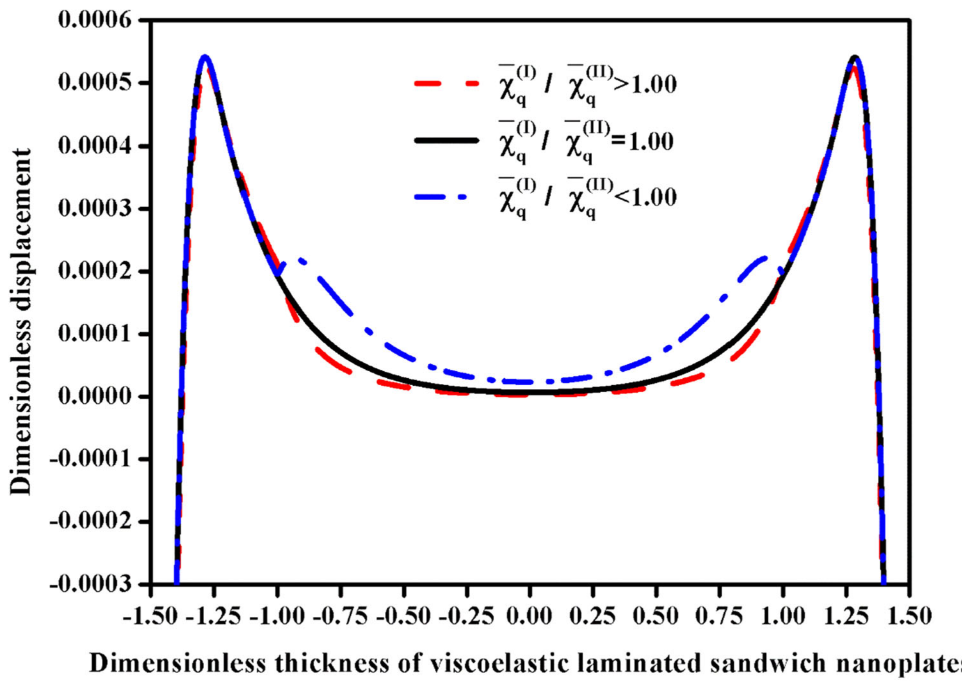

(b)

Fig. 4 continued

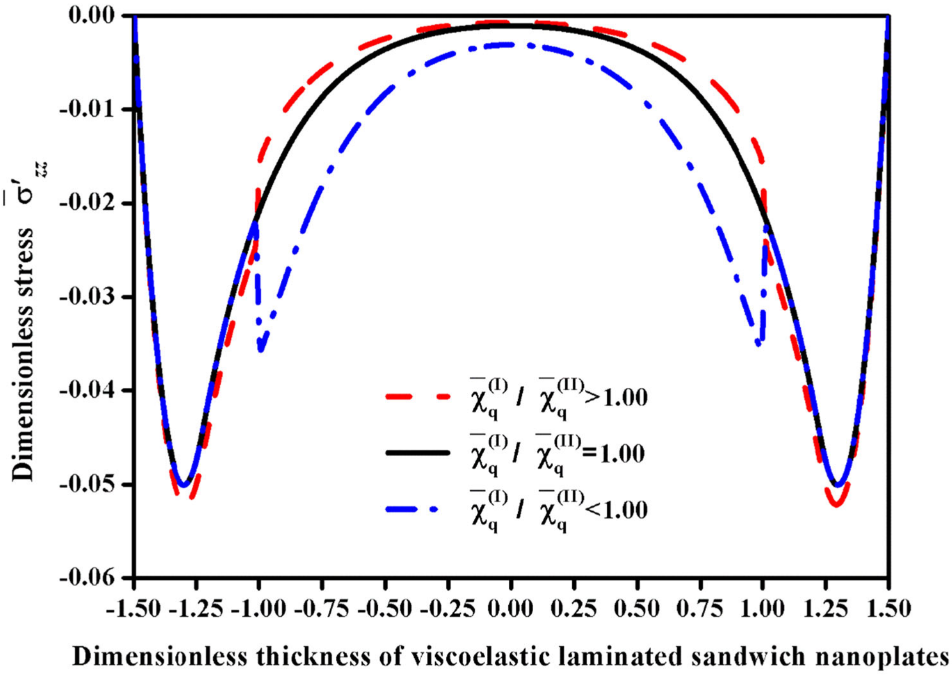

(c)

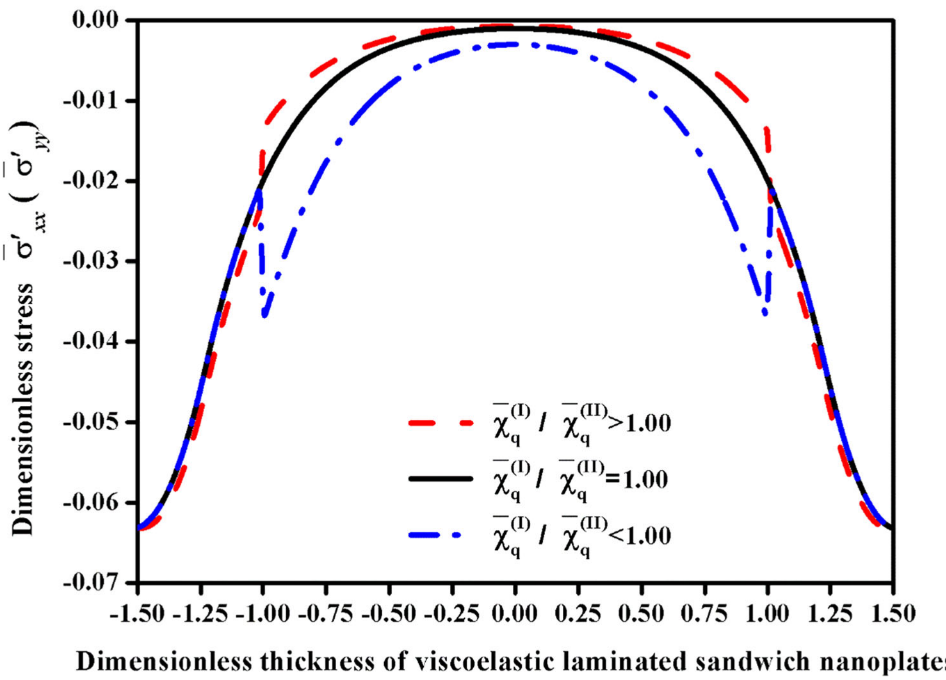

(d)

Fig. 5 Dimensionless results for $\overline{e}_0\overline{a}^{(\mathrm{I})} = \overline{e}_0\overline{a}^{(\mathrm{II})} = \overline{e}_0\overline{a}^{(\mathrm{III})} = \overline{e}_0\overline{a}^{(i)}$

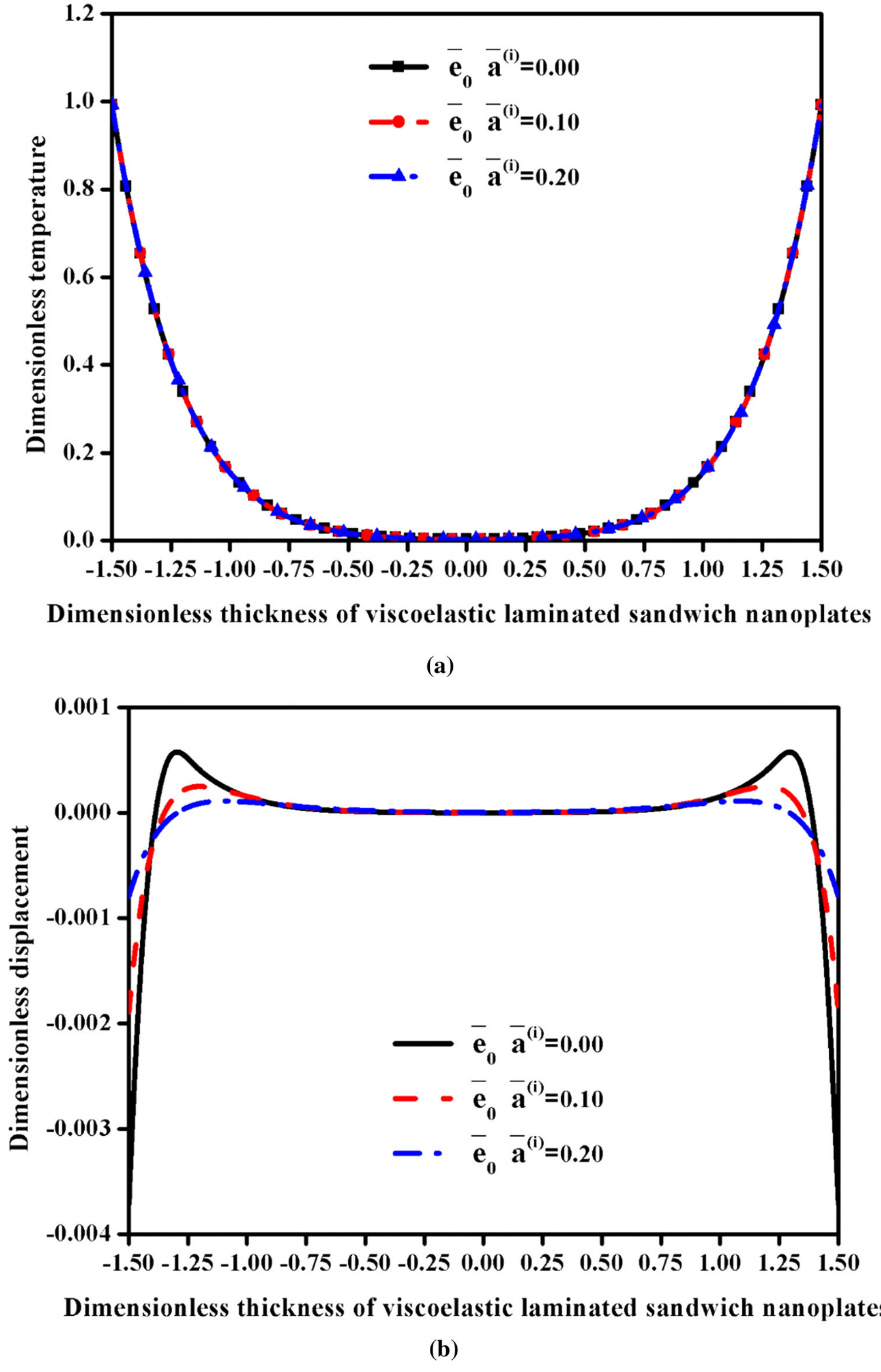

Fig. 5 continued

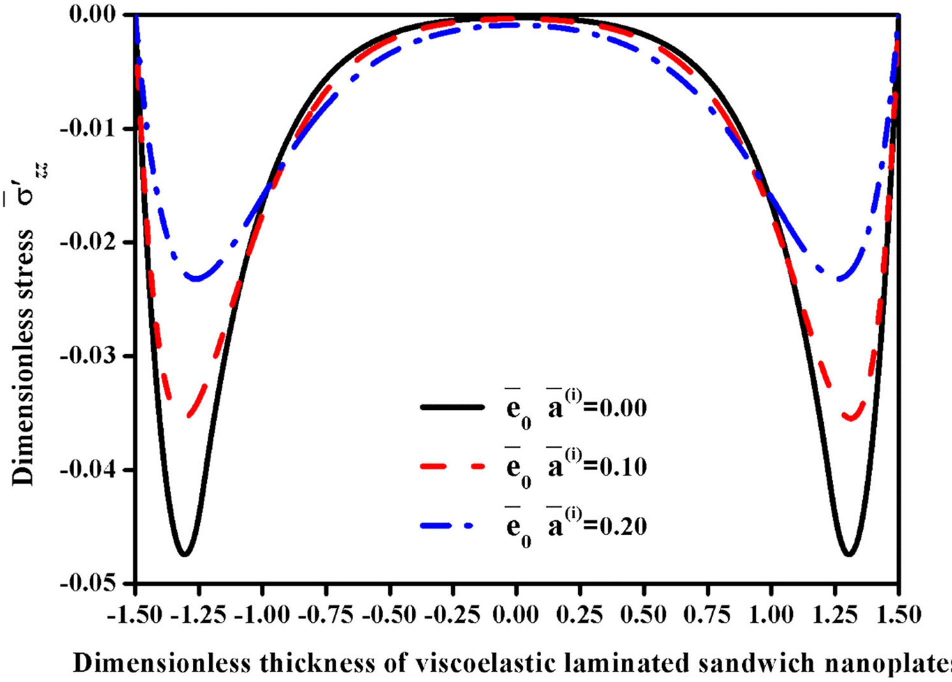

(c)

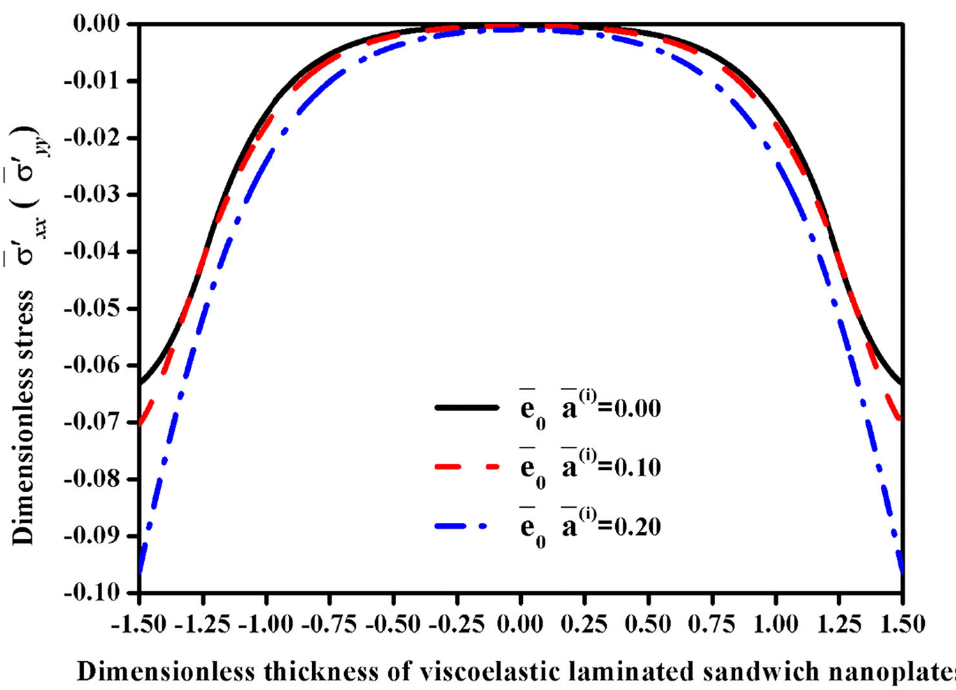

(d)

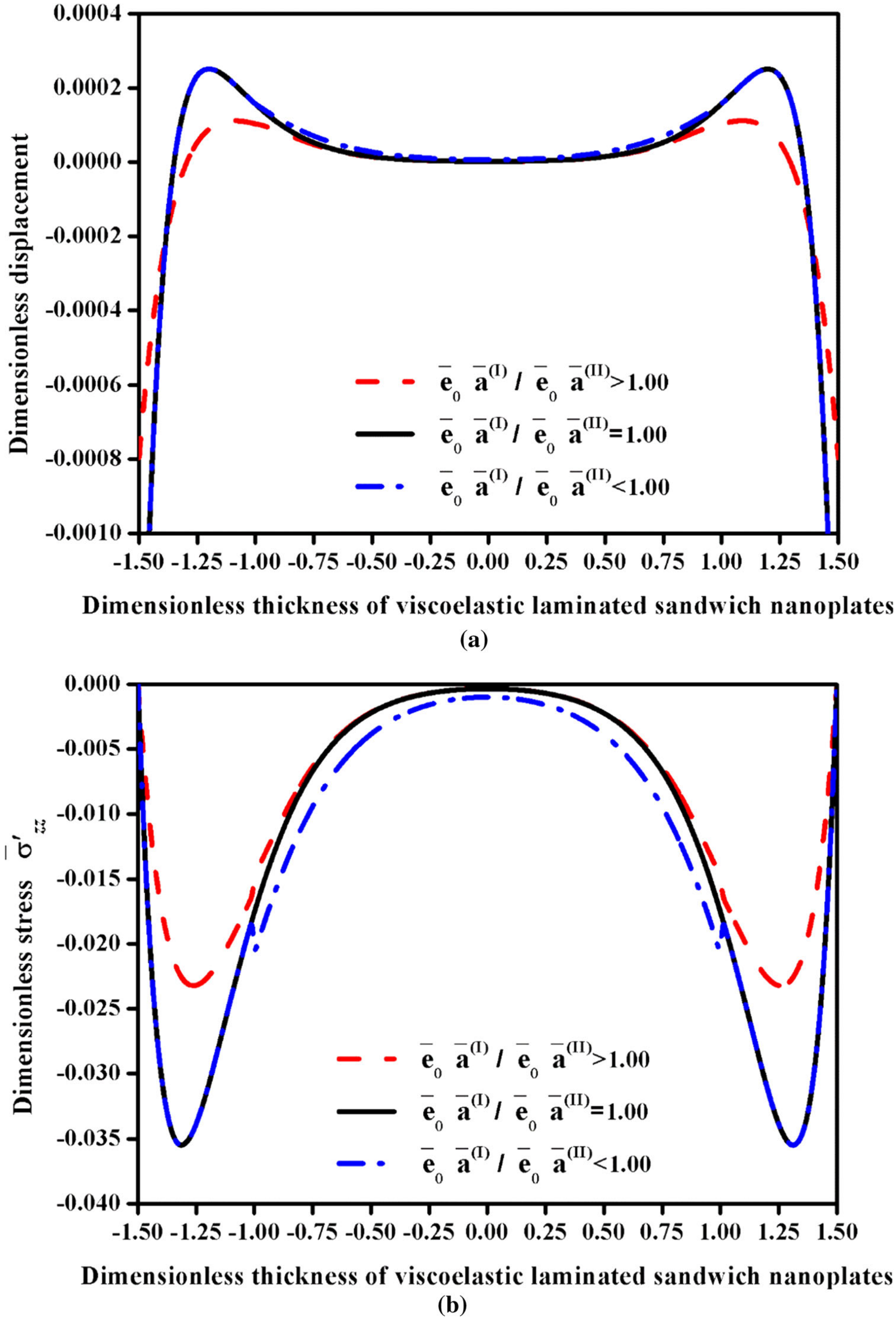

Fig. 6 Dimensionless results for different combinations of $\overline{e}_0\overline{a}^{(i)}$

the case of $\overline{\chi}_q^{(\mathrm{I})}\Big/\overline{\chi}_q^{(\mathrm{II})} > 1.00$ is beneficial to the heat and harmful thermal-induced stress isolation.

4.2 The effect of elastic nonlocal parameter $\overline{e}_0\overline{a}^{(i)}$

Figures 5 and 6 present the structural dynamic responses for different selections of elastic nonlocal parameter when

Fig. 6 continued

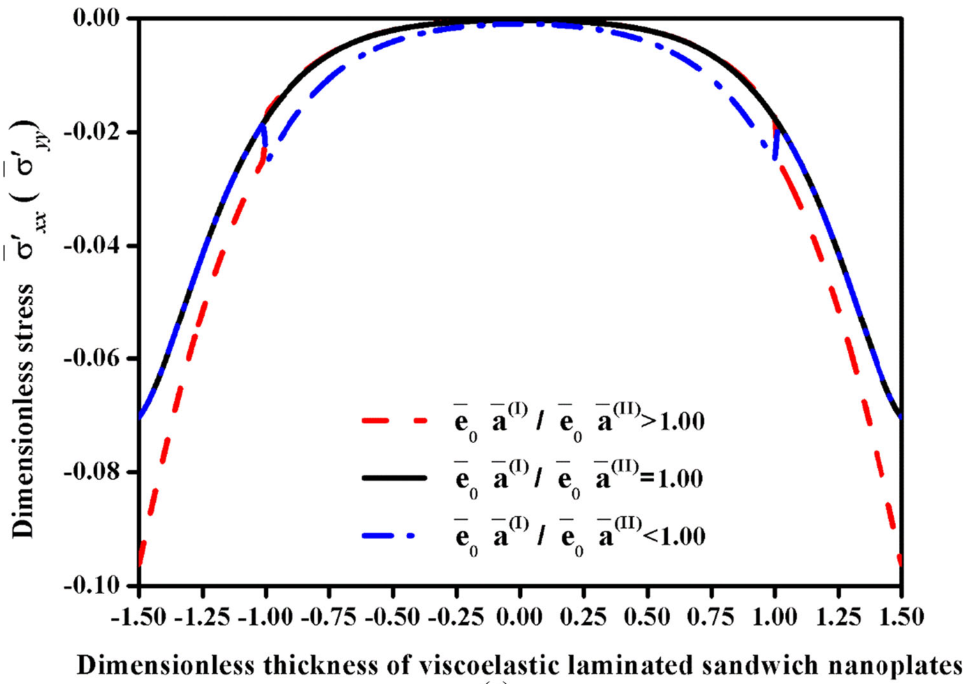

(c)

$\overline{\chi}_q^{(i)} = 0$. In the case of $\overline{e}_0\overline{a}^{(\mathrm{I})}/\overline{e}_0\overline{a}^{(\mathrm{II})} = 1$, one can observed that: (i) the temperature response for $\overline{e}_0\overline{a}^{(i)} = 0.10$ or $\overline{e}_0\overline{a}^{(i)} = 0.20$ agrees well with that for $\overline{e}_0\overline{a}^{(i)} = 0.00$. This suggests that $\overline{e}_0\overline{a}^{(i)}$ has no effect on the distribution of temperature; (ii) the Medium I and III will deform smaller, and the distribution of displacement becomes even smoother; (iii) the compressive stress $\bar{\sigma}'_{zz}$ is lower in Medium I and III, but higher in Medium II; (iv) the compressive stress $\bar{\sigma}'_{xx}$ ($\bar{\sigma}'_{yy}$) is improved in Medium I, II and III; (v) the displacement is reduced at $\overline{z} = \pm 0.50$, but the compressive stress $\bar{\sigma}'_{xx}$ ($\bar{\sigma}'_{yy}$) will become larger. Figure 6 displayed dimensionless results under different combinations of $\overline{e}_0\overline{a}^{(i)}$. If $\overline{e}_0\overline{a}^{(\mathrm{I})}/\overline{e}_0\overline{a}^{(\mathrm{II})} > 1.00$, it can be concluded that: (i) the absolute values of displacement in Medium I, II and III will be decreased, even at $\overline{z} = \pm 0.50$; (ii) the compressive stress $\bar{\sigma}'_{zz}$ will be greatly reduced in Medium I and III, but not changed in Medium II; (iii) the compressive stress $\bar{\sigma}'_{xx}$ ($\bar{\sigma}'_{yy}$) increases in Medium I and III, whilst it suddenly jumps from a higher value to a lower one at $\overline{z} = \pm 0.50$. If $\overline{e}_0\overline{a}^{(\mathrm{I})}/\overline{e}_0\overline{a}^{(\mathrm{II})} < 1.00$, the distribution of displacement is almost unchanged in Medium I and III, but Medium II will deform larger. On the other hand, the compressive stress $\bar{\sigma}'_{zz}$ or $\bar{\sigma}'_{xx}$ ($\bar{\sigma}'_{yy}$) is not changed in Medium I and III, but it abruptly jumps to a higher value at $\overline{z} = \pm 0.50$, whilst the magnitudes of compressive stress become larger in Medium II. The results may be useful for practical applications: if the ratio of $\overline{e}_0\overline{a}^{(\mathrm{I})}/\overline{e}_0\overline{a}^{(\mathrm{II})} < 1.00$ is taken, the ability of stress isolation will be improved.

4.2.1 The effects of material constants ratios

This subsection mainly contributes to analyze and discuss the effects of material constants ratios on the structural thermo-viscoelastic responses if following conditions are always satisfied: $\overline{\chi}_q^{(i)}$=0.10, $\overline{e}_0\overline{a}^{(i)} = 0.10$.

4.2.2 The effect of relaxation function ratio

Figure 7 is displayed for the dynamic responses under different combinations of relaxation function. If the relaxation function in Medium I or III is larger than that in Medium II, i.e. $R^{(\mathrm{I})}/R^{(\mathrm{II})} > 1.00$, one can observe that: (i) the temperature response is not changed in Medium I and III, but it becomes larger in Medium II; (ii) the Medium II will deform smaller; (iii) the compressive stress $\bar{\sigma}'_{zz}$ decreases in Medium I, II and III; (iv) the compressive stress $\bar{\sigma}'_{xx}$ ($\bar{\sigma}'_{yy}$) is improved in Medium I and III, but reduced in Medium II; (v) the temperature or compressive stress will abruptly jump to a lower value at $\overline{z} = \pm 0.50$. If the ratio of $R^{(\mathrm{I})}/R^{(\mathrm{II})} < 1.00$ is adopted, Fig. 7 shows that the responses of temperature, displacement and compressive stresses increase in Medium II. Clearly, the absolute values of temperature and compressive stresses will be suddenly improved to higher values at $\overline{z} = \pm 0.50$. It can be concluded that the abilities of heat and harmful stresses isolation can be efficiently lifted in the case of $R^{(\mathrm{I})}/R^{(\mathrm{II})} > 1.00$.

Fig. 7 Dimensionless results for different relaxation function ratio

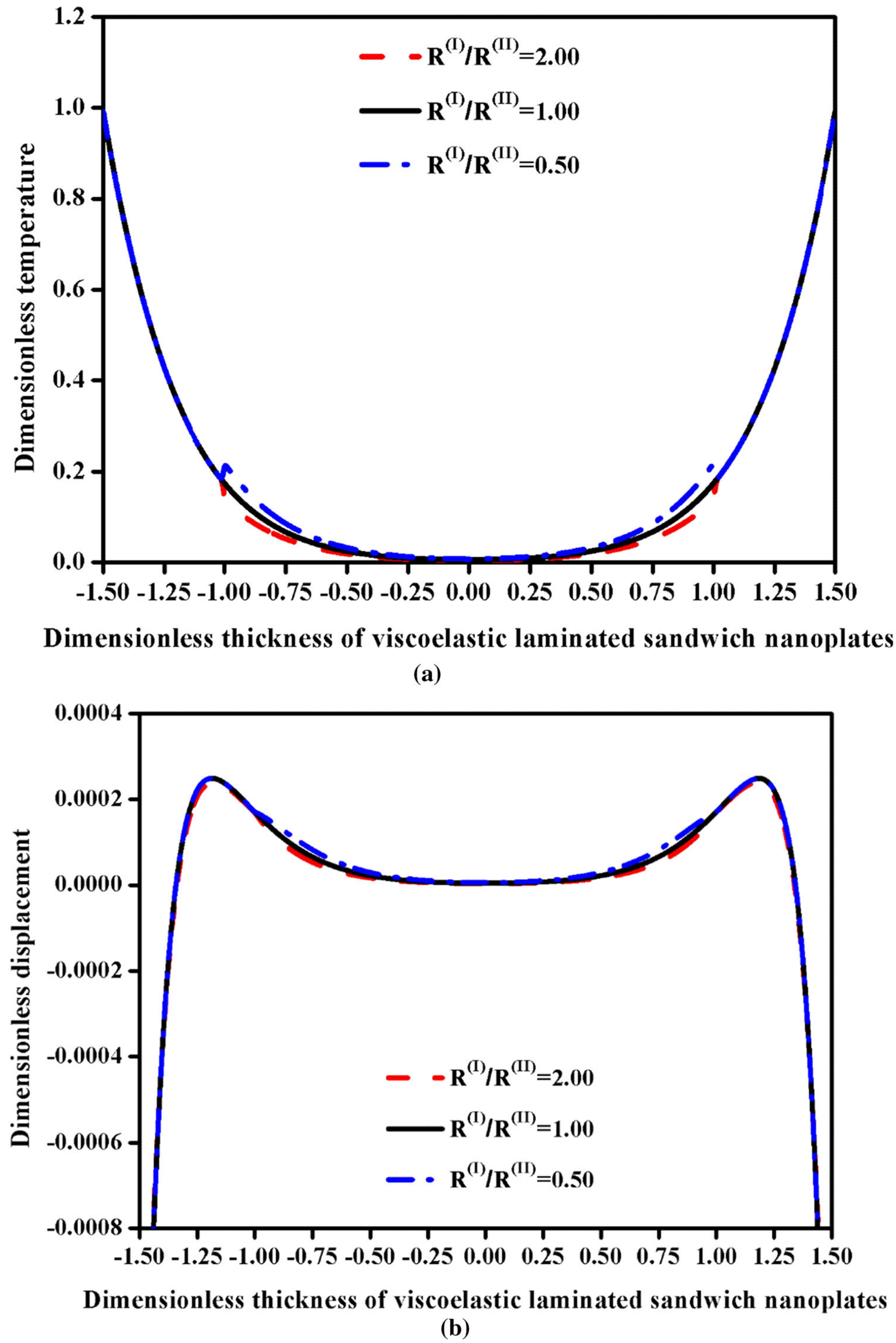

4.2.3 The effect of bulk modulus ratio

As illustrated in Fig. 8, the effect of bulk modulus ratio on the responses is evaluated and discussed. Firstly, the temperature response is not changed in the case of $\beta^{(I)}\Big/\beta^{(II)} > 1.00$, $\beta^{(I)}\Big/\beta^{(II)} = 1.00$ or $\beta^{(I)}\Big/\beta^{(II)} < 1.00$. This indicates that the bulk modulus ratio has no effect on the distribution of temperature response. Secondly, if $\beta^{(I)}\Big/\beta^{(II)} > 1.00$, it is clearly observed that: (i) the displacement response is not changed in Medium II, while Medium I and III will deform smaller, even at $\bar{z} = \pm 0.50$; (ii) the compressive stresses $\bar{\sigma}'_{zz}$ and $\bar{\sigma}'_{xx}$ ($\bar{\sigma}'_{yy}$) become lower in Medium I and III, but almost unchanged in Medium II;

Fig. 7 continued

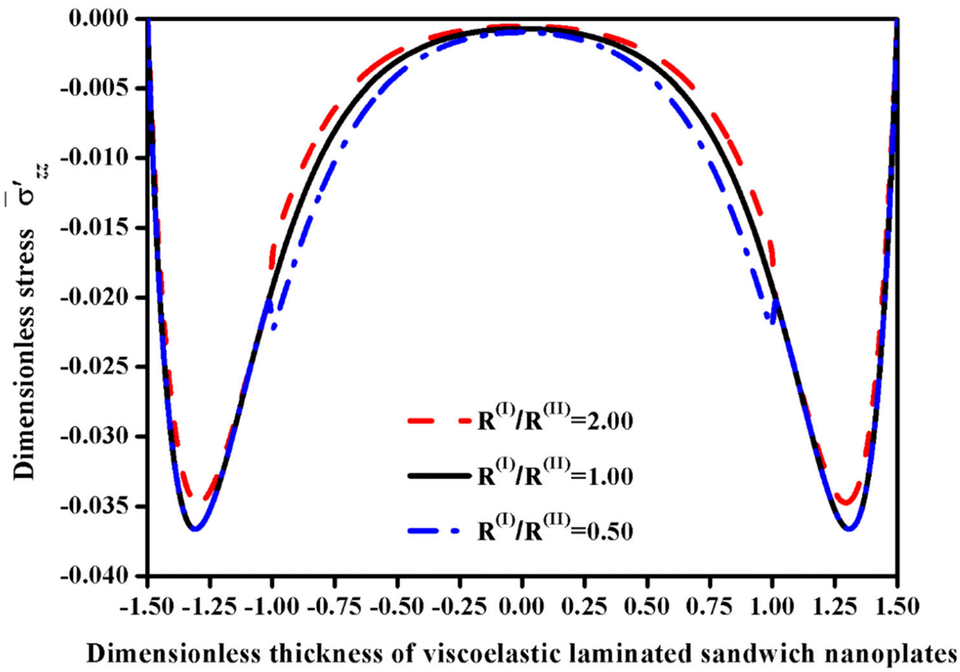

(c)

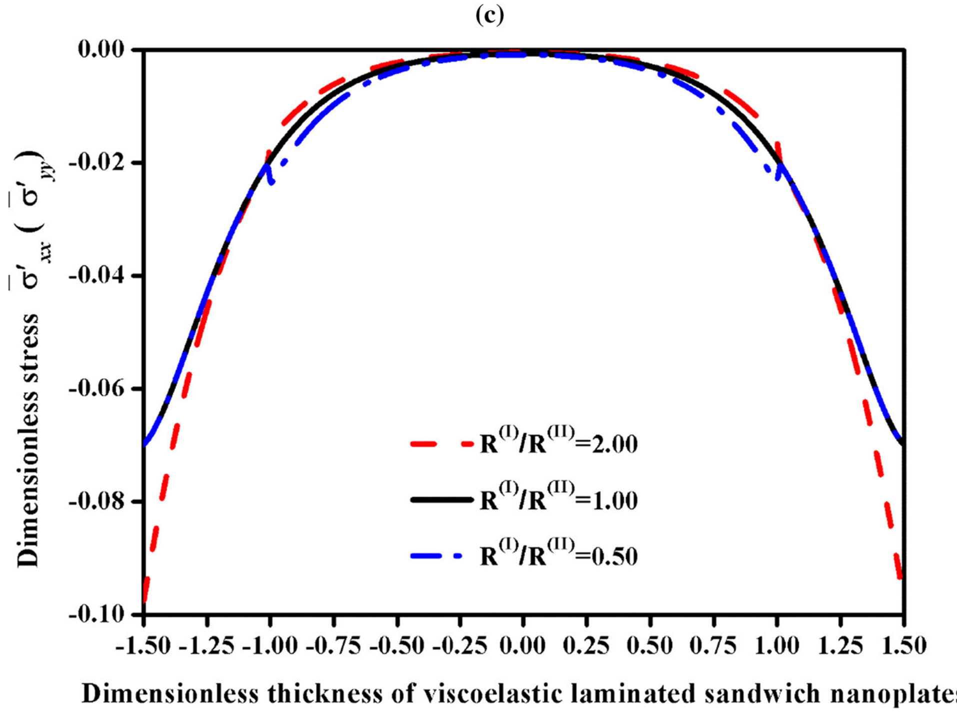

(b)

(iii) the compressive stress $\bar{\sigma}'_{zz}$ or $\bar{\sigma}'_{xx}$ ($\bar{\sigma}'_{yy}$) will suddenly jump form a higher response to a lower one at $\bar{z} = \pm 0.50$. Thirdly, if $\beta^{(\mathrm{I})} \big/ \beta^{(\mathrm{II})} < 1.00$, it is seen that: (i) the distribution of displacement is not changed in Medium I or III, whereas Medium II deforms smaller; (ii) the compressive stresses $\bar{\sigma}'_{zz}$ or $\bar{\sigma}'_{xx}$ ($\bar{\sigma}'_{yy}$) increases in Medium II, and it will be greatly improved to a higher value at $\bar{z} = \pm 0.50$. Clearly, the compressive stresses are significantly reduced, which suggests that stress isolation will be greatly improved.

4.2.4 The effect of thermal conductivity ratio

Shown in Fig. 9, the dimensionless results of structural dynamic responses are graphically illustrated for different

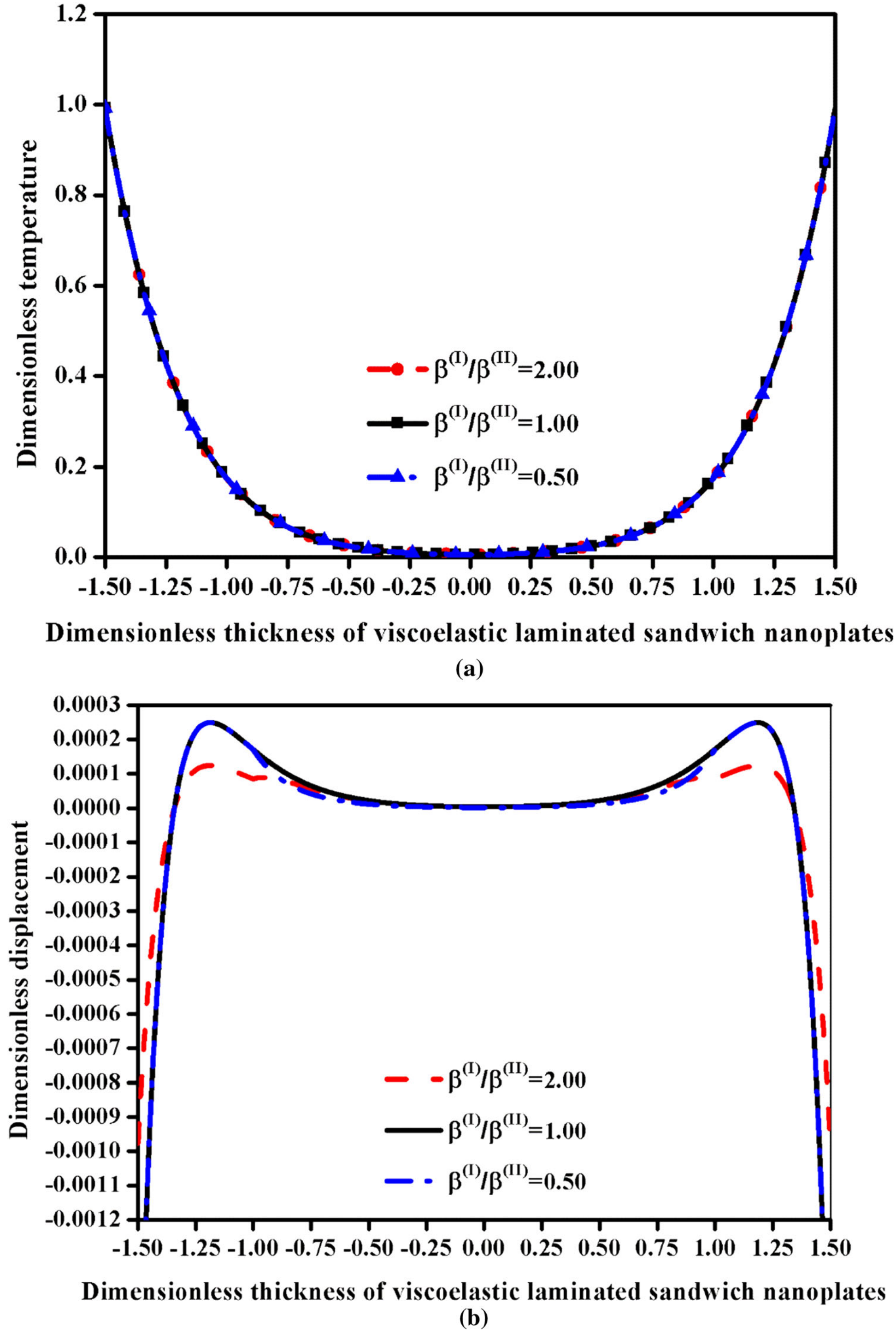

Fig. 8 Dimensionless results for different bulk modulus ratio

ratios of thermal conductivity. From Fig. 9, it is indicated that all the responses for $\kappa^{(\mathrm{I})}/\kappa^{(\mathrm{II})} > 1.00$ and $\kappa^{(\mathrm{I})}/\kappa^{(\mathrm{II})} < 1.00$ match well with those for $\kappa^{(\mathrm{I})}/\kappa^{(\mathrm{II})} = 1.00$. This suggests that the distribution of temperature, displacement and compressive stresses will not be affected by the ratio of $\kappa^{(\mathrm{I})}/\kappa^{(\mathrm{II})}$. If $\kappa^{(\mathrm{I})}/\kappa^{(\mathrm{II})} > 1.00$, the temperature in Medium II will increase, whilst the absolute value of displacement becomes larger. In such a case, the compressive stresses $\bar{\sigma}'_{zz}$ and $\bar{\sigma}'_{xx}$ ($\bar{\sigma}'_{yy}$) increase. Additionally, the temperature or compressive stress abruptly jumps from a lower value to a higher one at

Fig. 8 continued

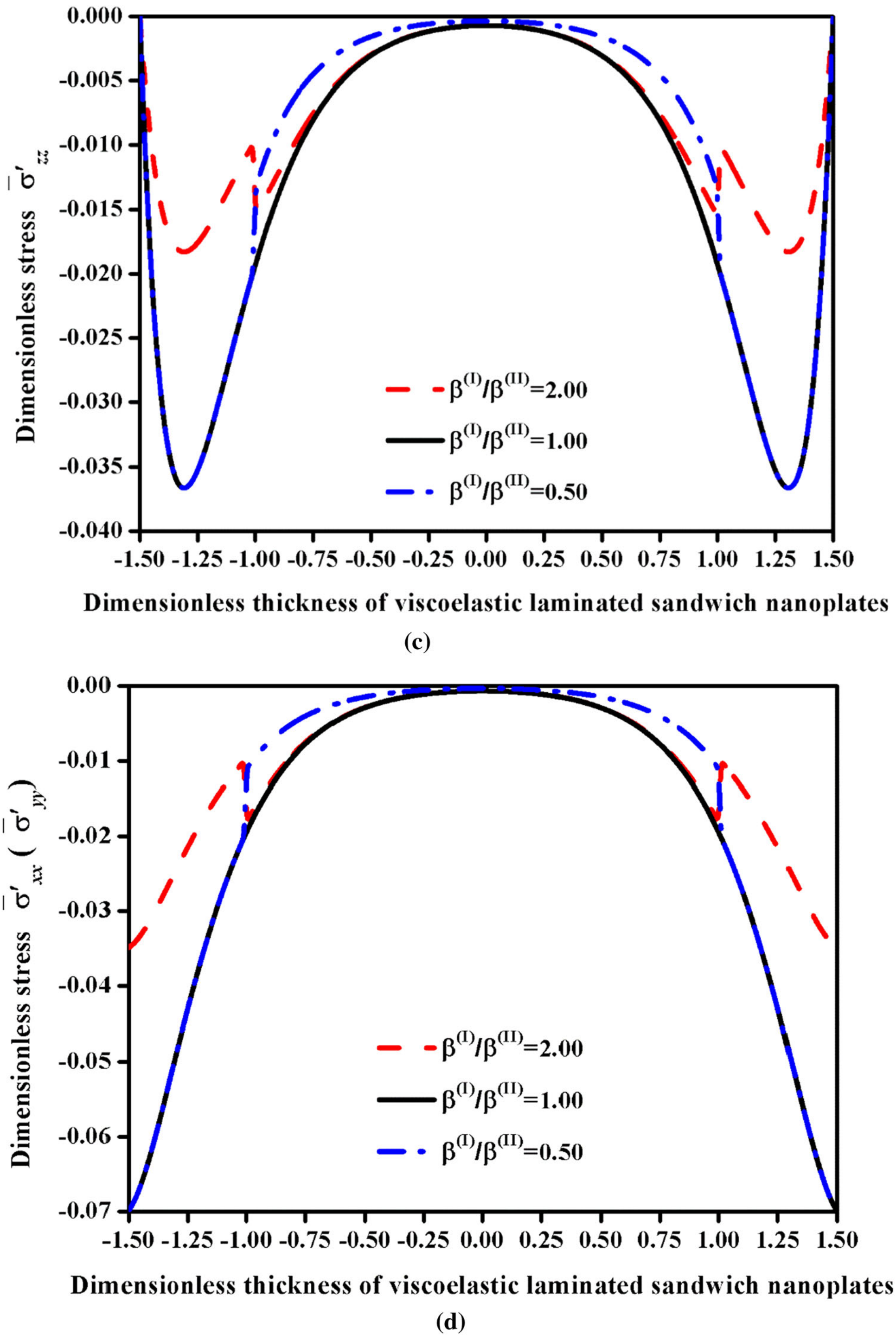

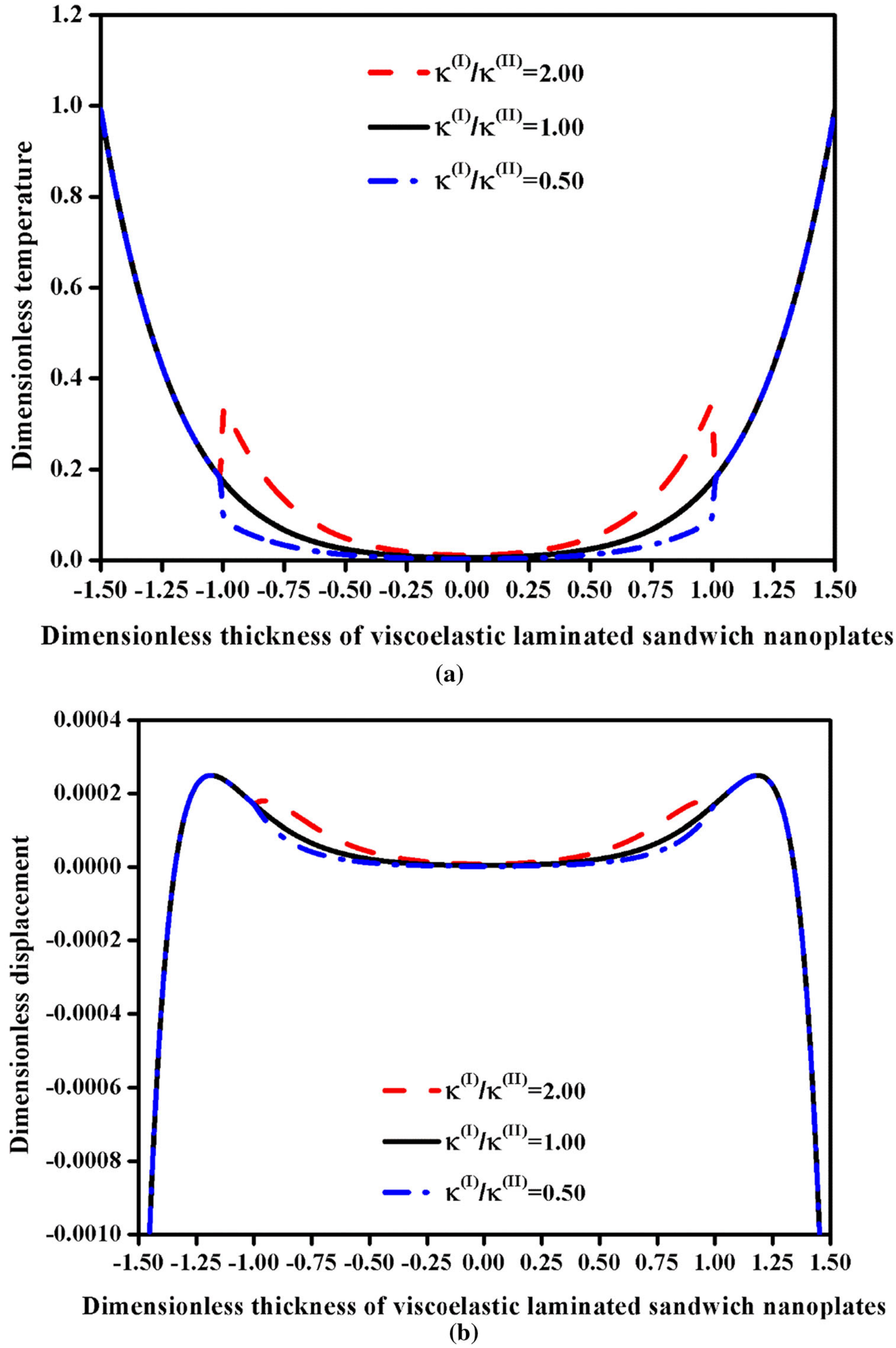

Fig. 9 Dimensionless results for different thermal conductivity ratio

Fig. 9 continued

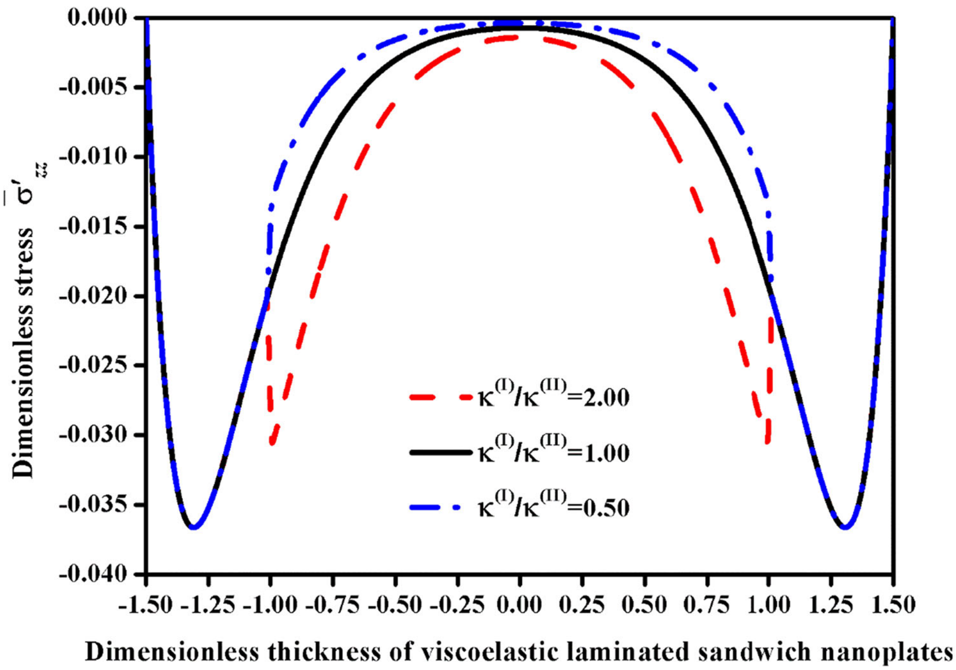

(c)

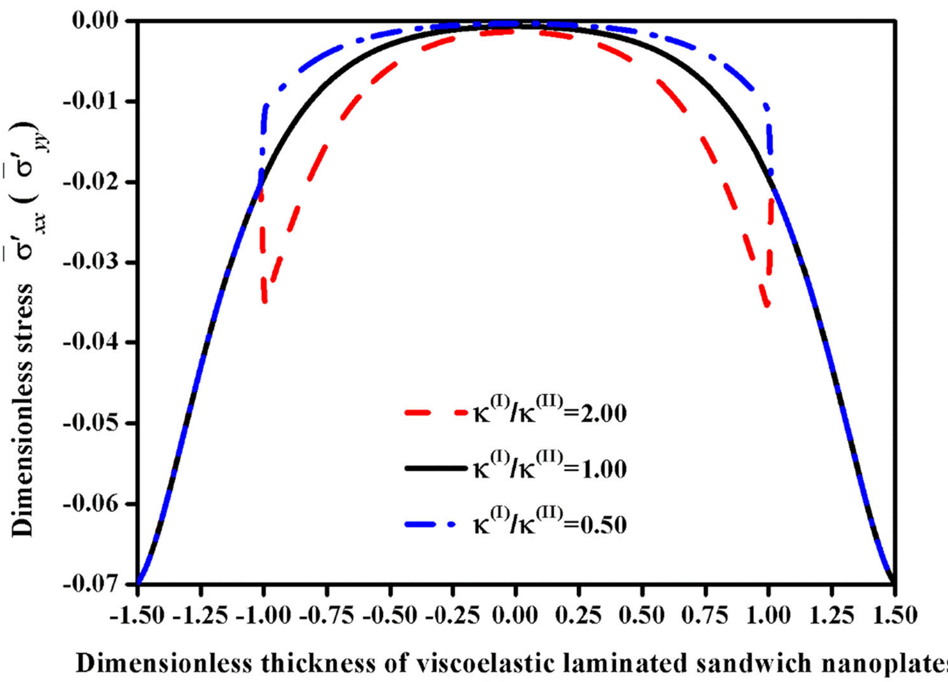

(d)

$\bar{z} = \pm 0.50$. If $\kappa^{(\mathrm{I})}/\kappa^{(\mathrm{II})} < 1.00$, the temperature decreases in Medium II, and the displacement is accordingly reduced. Consequently, the compressive stress $\bar{\sigma}'_{zz}$ or $\bar{\sigma}'_{xx}$ ($\bar{\sigma}'_{yy}$) decreases. The sharp jumps of temperature and compressive stress at $\bar{z} = \pm 0.50$ will be lowered. From above discussion, it can be deduced that the heat and stress isolation at the surface coatings of the structure will be improved in the case of $\kappa^{(\mathrm{I})}/\kappa^{(\mathrm{II})} < 1.00$.

5 Concluding remarks

A complete nonlocal thermo-viscoelasticity model (Li et al. 2021a) has been developed to fully consider the size effects of elastic deformation and heat transfer, which paves a new important branch in this research field. However, in view of current studies, there are no works have contributed on structural dynamic responses of layer-by-layer viscoelastic sandwich nanocomposites subjected to time-varying symmetric thermal shock loadings based on this theory. Following the theory (Li et al. 2021a), this work aims to deal with this problem by developing an analytical model and obtain the time-domain solutions by a semi-analytical technique via Laplace transformation. The numerical results show that:

(i). The increase of thermal nonlocal parameter will reduce heat and stress isolation for the surface coatings at the interfaces.

(ii). The increase of elastic nonlocal parameter will improve the absolute value of compressive stresses, while the sandwich nanoplates will deform smaller and the distribution of displacement becomes even smoother.

(iii). Different combinations of thermal and elastic nonlocal parameters can improve the ability of heat and stress isolation to some extent.

(iv). Properly selecting material constants ratios will remarkably affect the structural dynamic thermo-viscoelastic responses and lift the heat and stress isolation

This paper is expected to provide a thorough and comprehensive understanding on nonlocal thermo-viscoelastic responses of layer-by-layer viscoelastic sandwich nanocomposites. The strategy and achieved results in present work will present some basic guidelines for its strength design and vibration control.

Acknowledgements This work is supported by the National Natural Science Foundation of China (11972176, 1210021715), the Young Science and Technology Talents Lift Project of Gansu Province, the Natural Science Foundation of Gansu Province (21JR1RA241), the Opening Project from the State Key Laboratory for Strength and Vibration of Mechanical Structures (SV2019-KF-30), and Tianyou Youth Talent Lift Program of Lanzhou Jiaotong University.

Declarations

Conflict of interest We declare that we have no conflict of interest.

References

Akbarov SD, Yahnioglu N, Tekin A (2014) Buckling delamination of a rectangular viscoelastic sandwich plate containing interface inner cracks. J Eng Mech 140:134–148

Barretta R, de Sciarra FM (2018) Constitutive boundary conditions for nonlocal strain gradient elastic nano-beams. Int J Eng Sci 130:187–198

Biswas S (2020) Three-dimensional nonlocal thermoelasticity in orthotropic medium based on Eringen's nonlocal elasticity. Waves Rand Complex Med. https://doi.org/10.1080/17455030.2020.1810366

Brancik L (1999) Programs for fast numerical inversion of laplace transforms in MATLAB language environment. Proc Seventh Prague Conf MATLAB 99:27–39

Cao BY, Guo ZY (2007) Equation of motion of a phonon gas and non-Fourier heat conduction. J Appl Phys 102:053503

Chan WL, Averback RS, Cahill DG, Lagoutchev A (2008) Dynamics of femtosecond laser-induced melting of silver. Phys Rev B 78:214107

Chen G (2001) Ballistic-diffusive heat-conduction Equations. Phys Rev Lett 86:2297–2300

Dowlati S, Rezazadeh G (2018) A new approach to the evaluation of Casimir and van der Waals forces in the transition region. Chin J Phys 56:1133–1146

Eringen AC (1972) Linear theory of nonlocal elasticity and dispersion of plane waves. Int J Eng Sci 10:425–435

Eringen AC (1983) On differential equations of nonlocal elasticity and solutions of screw dislocation and surface waves. J Appl Phys 54:4703–4710

Eringen AC (2002) Nonlocal continuum field theories. Springer, New York

Fan F, Kiani K (2021) A rigorously analytical exploration of vibrations of arbitrarily shaped multi-layered nanomembranes from different materials. Int J Mech Sci 206:106603

Govindjee S, Sackman JL (1999) On the use of continuum mechanics to estimate the properties of nanotubes. Solid State Commun 110:227–230

Guo ZY, Hou QW (2010) Thermal wave based on the thermomass model. J Heat Transfer 7:072403

Guo HL, He TH, Tian XG, Shang FL (2021) Size-dependent mechanical-diffusion responses of multilayered composite nanoplates. Waves Random Complex Media 31:2355–2384

Guo HL, Shang FL, Tian XG, Zhang H (2021) Size-dependent generalized thermo-viscoelastic response analysis of multilayered viscoelastic laminated nanocomposite account for imperfect interfacial conditions. Waves Random Complex Media. https://doi.org/10.1080/17455030.2021.1917793

Gurtin ME, Sternberg E (1962) On the liner theory of viscoelasticity. Arch Ration Mech Anal 11:291–356

Guyer RA, Krumhans JA (1966) Solutions of linearized phonon Boltzmann equation. Phys Rev 148:765–778

Hoogeboom-Pot KM, Hernandez-Charpak JN, Gu XK, Frazer TD, Anderson EH, Chao WL, Falcone RW, Yang RG, Murnane MM, Kapteyn HC, Nardi D (2015) A new regime of nanoscale thermal

transport: collective diffusion increases dissipation efficiency. PANS 112:4846–4851
Hosseini M, Bahreman M, Jamalpoor A (2017) Thermomechanical vibration analysis of FGM viscoelastic multi-nanoplate system incorporating the surface effects via nonlocal elasticity theory. Microsyst Technol 23:3041–3058
Jou D, Lebon G, Criado-Sancho M (2010) Variational principles for thermal transport in nanosystems with heat slip flow. Phys Rev E 82:031128
Karami B, Shahsavari D (2019) Nonlocal strain gradient model for thermal stability of FG nanoplates integrated with piezoelectric layers. Smart Struct Syst 23:215–225
Kiani K (2016) Thermo-mechanical analysis of functionally graded plate-like nanorotors: a surface elasticity model. Int J Mech Sci 106:39–49
Kiani K (2016a) Elasto-dynamic analysis of spinning nanodisks via a surface energy-based model. J Phys D Appl Phys 49:275306
Kiani K (2017) In-plane vibration and instability of nanorotors made from functionally graded materials accounting for surface energy effect. Microsyst Technol 23:4853–4869
Kolahchi R (2017) A comparative study on the bending, vibration and buckling of viscoelastic sandwich nano-plates based on different nonlocal theories using DC, HDQ and DQ methods. Aerosp Sci Technol 66:235–248
Kolahchi R, Hosseini H, Esmailpour M (2016) Differential cubature and quadrature-bolotin methods for dynamic stability of embedded piezoelectric nanoplates based on visco-nonlocal-piezoelasticity theories. Compos Struct 157:174–186
Lei Y, Adhikari S, Friswell MI (2013) Vibration of nonlocal Kelvin–Voigt viscoelastic damped Timoshenko beams. Int J Eng Sci 66:1–13
Li L, Hu YJ (2015) Buckling analysis of size-dependent nonlinear beams based on a nonlocal strain gradient theory. Int J Eng Sci 97:84–94
Li L, Hu YJ (2016) Wave propagation in fluid-conveying viscoelastic carbon nanotubes based on nonlocal strain gradient theory. Comput Mater Sci 112:282–288
Li YH, Dong YH, Qin Y, Lv HW (2018) Nonlinear forced vibration and stability of an axially moving viscoelastic sandwich beam. Int J Mech Sci 138:131–145
Li CL, Guo HL, Tian XG (2019) Nonlocal second-order strain gradient elasticity model and its application in wave propagation in carbon nanotubes. Microsyst Technol 25:2215–2227
Li CL, Guo HL, Tian XG, He TH (2019b) Size-dependent thermo-electromechanical responses analysis of multilayered piezoelectric nanoplates for vibration control. Compos Struct 225:111112
Li CL, Tian XG, He TH (2021a) Nonlocal thermo-viscoelasticity and its application in size-dependent responses of bi-layered composite viscoelastic nanoplate under nonuniform temperature for vibration control. Mech Adv Mater Struct 28:1797–1811
Li CL, Guo HL, Tian XG, He TH (2021b) Nonlocal diffusion-elasticity based on nonlocal mass transfer and nonlocal elasticity and its application in shock-induced responses analysis. Mech Adv Mater Struct 28:827–838
Li CL, He TH, Tian XG (2022) Nonlocal theory of thermoelastic diffusive materials and its application in structural dynamic thermo-elasto-diffusive responses analysis. Waves Random Complex Media 32:174–203
Lim CW, Zhang G, Reddy JN (2015) A higher-order nonlocal elasticity and strain gradient theory and its applications in wave propagation. J Mech Phys Solids 78:298–313
Lu JP (1997) Elastic properties of carbon nanotubes and nanoropes. Phys Rev Lett 79:1297–1300
Mahmoudpour E, Hosseini-Hashemi SH, Faghidian SA (2018) A nonlocal strain gradient theory for nonlinear free and forced vibration of embedded thick FG double layered nanoplates. Struct Eng Mech 68:103–119
Mindlin R (1965) Second gradient of strain and surface-tension in linear elasticity. Int J Solids Struct 1:414–438
Polizzotto C (2014) Stress gradient versus strain gradient constitutive models within elasticity. Int J Solids Struct 51:1809–1818
Pradhan SC, Phadikar JK (2009) Nonlocal elasticity theory for vibration of nanoplates. J Sound Vib 325:206–223
Reddy JN (2007) Nonlocal theories for bending, buckling and vibration of beams. Int J Eng Sci 45:288–307
Romano G, Barretta R (2017) Nonlocal elasticity in nanobeams: the stress-driven integral model. Int J Eng Sci 115:14–27
Romano G, Barretta R, Diaco M, de Sciarra FM (2017) Constitutive boundary conditions and paradoxes in nonlocal elastic nanobeams. Int J Mech Sci 121:151–156
Shahrbabaki EA (2018) On three-dimensional nonlocal elasticity: free vibration of rectangular nanoplate. Eur J Mech A Solids 71:122–133
Sheng M, Guo Z, Qin Q, He Y (2018) Vibration characteristics of a sandwich plate with viscoelastic periodic cores. Compos Struct 206:54–69
Soboley SL (1994) Equations of transfer in non-local media. Int J Heat Mass Transf 37:2175–2182
Tzou DY, Guo ZY (2010) Nonlocal behavior in thermal lagging. Int J Therm Sci 49:1133–1137
Yang F, Chong ACM, Lam DCC, Tong P (2002) Couple stress based strain gradient theory for elasticity. Int J Solids Struct 39:2731–2743
Yu YJ, Tian XG, Xiong QL (2016) Nonlocal thermoelasticity based on nonlocal heat conduction and nonlocal elasticity. Eur J Mech A Solids 60:238–253
Zhou XQ, Yu DY, Shao XY, Zhang SQ, Wang S (2016) Research and applications of viscoelastic vibration damping materials: a review. Compos Struct 136:460–480
Zhu XW, Li L (2017) Twisting statics of functionally graded nanotubes using Eringen's nonlocal integral model. Compos Struct 178:87–96